Chemical Vapor Deposition Models Using Direct Simulation Monte Carlo with Non-Linear Chemistry and Level Set Profile Evolution

By

Husain Ali Al-Mohssen

Bachelor of Science in Mechanical Engineering
KFUPM, Saudi Arabia
(1998)

SUBMITTED TO THE DEPARTMENT OF MECHANICAL ENGINEERING IN PARTIAL FULFILLMENT OF THE REQUIREMENTS FOR THE DEGREE OF MASTER OF SCIENCE IN MECHANICAL ENGINEERING

At the

MASSACHUSETTS INSTITUTE OF TECHNOLOGY

September 2003

Signature of Author ……...
Department of Mechanical Engineering
July 1, 2003

Certified by…….……...
Nicolas G. Hadjiconstantinou
Rockwell International Associate Professor of Mechanical Engineering

Accepted by ……..……...
Ain A. Sonin
Chairman, Department Committee on Graduate Students

This page is Intentionally Left Blank

Chemical Vapor Deposition Models Using Direct Simulation Monte Carlo With Non-Linear Chemistry and Level Set Profile Evolution

By

Husain Ali Al-Mohssen

Submitted to the department of Mechanical Engineering in partial fulfillment of the retirements for the degree of Master of Science in Mechanical Engineering

Abstract

In this work we use the Direct Simulation Monte Carlo (DSMC) method to simulate Chemical Vapor Deposition (CVD) in small scale trenches. Transport in the gas is decoupled from the boundary movement by assuming that the two processes evolve at different timescales. Consequently, the deposition problem is solved by the successive application of a DSMC gas transport model and a boundary movement model.

The DSMC gas transport model used is standard with the exception of the ability to model arbitrarily shaped 2D surface boundaries. In addition, a method is proposed and used to incorporate non-linear reaction rate correlations into the gas surface interaction. Our DSMC results of the complete model are extensively compared to analytical and theoretical results to validate the approach and the implementation.

The Level Set method is incorporated in our work to produce a sophisticated boundary movement model. This model is also verified by comparing our results to published results. Finally, concepts form the Level Set methodology were used to dramatically improve the performance of the DMSC transport model when dealing with complex boundaries at low Knudsen Numbers.

Thesis Supervisor: Dr. N. G. Hadjiconstantinou

Title: Associate Professor of Mechanical Engineering.

This page is intentionally left blank.

Acknowledgements:

All real thanks go to God for creating the reasons that allowed me to get to MIT and do this work. Other obvious thanks go to my wife for her help and patience over the last two years in our new life here in the US.

I would also like to give many thanks to Professor Hadjiconstantinou, my advisor, for his great help and immense patience with my (many) mistakes. I certainly look forward to working with him again for my Doctorate degree.

I would also like to acknowledge the great support of Dr. Wroble over the summer and fall months of last year. I am sure I would not have been able to make it this far without her help. In the lab, I would like to thank Sanith and Lowell for teaching me so much both in and out of the squash court.

Finally, I am grateful for the support of Hasan Sabri and Nizar Al-Khadra at Saudi Aramco for arranging financial support for my studies and to Professor Maher ElMasri for encouraging me to apply to MIT.

This page is intentionally left blank.

Table of Contents:

To my wife

CHAPTER 1: INTRODUCTION AND BACKGROUND

1.1 Introduction

Chemical Vapor Deposition (CVD) is a manufacturing process used for growing thin layers of deposited material on pre-existing surfaces. CVD is used in many industries but it is of predominant importance in the semi-conductor industry because it is one of the few processes that allow the creation of high quality thin layers of specialized materials on the micro-meter scale. Figure 1 shows a sketch of an underlying substrate that has a layer of material grown over it using CVD. In a typical integrated-circuit application the dimensions of these features would be in the micrometer scale and the trench would be created by photolithography or other similar etching processes. The deposited layer is usually required to be very uniform and free of voids and cracks (as much as possible). As such, much effort is expended into optimizing the manufacturing process to ensure that the resulting profiles are acceptable with minimum use of time and materials.

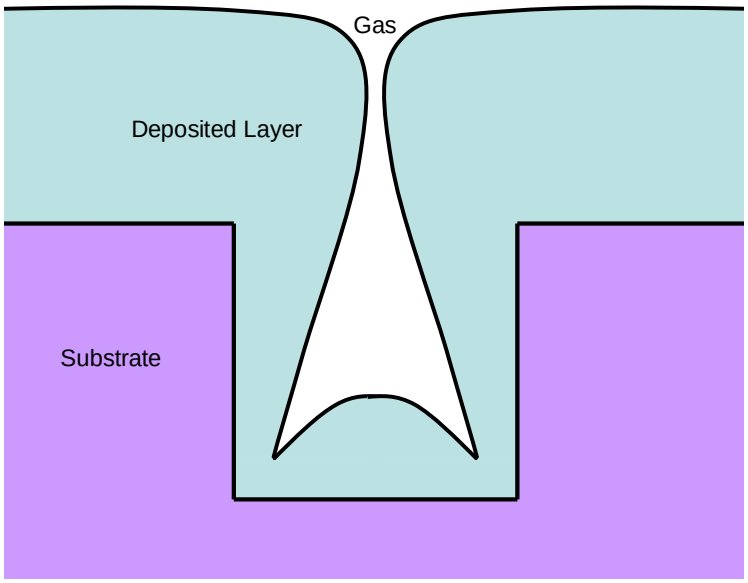

Figure 1: Illustration of layer growth over a substrate using chemical vapor deposition. Note the uneven thickness of the growth depending on the location along the trench.

The ability to accurately predict the shape of the deposited profile based on the process parameters is a very important factor in reducing CVD costs by reducing the guess-work associated with efficiently producing acceptable quality features that are free of voids or other non-uniformities. Other applications that need accurate CVD models include the extraction of reaction parameters of active species. In such applications measurements of deposition profiles are compared with profile predictions to extract values for reaction probabilities and other related properties.

1.2 Previous Work and Background

References [5] [6] [15] give a good overview of the CVD process and the manner in which accurate modeling of transport within the feature affects the ability to produce integrated circuits with acceptable properties and cost. The ratio of the mean free path of the gas above the trench being studied to the characteristic length of the feature is the single most important factor in determining which model to use in describing the growth of the deposition layer. This ratio is known as the *Knudsen Number* (Kn) and varies inversely with the overall pressure of the gas above the trench. The transport of the deposition molecules to the substrate varies from being collision dominated at high pressures ($Kn<<1$) to being exclusively determined by geometric factors and boundary conditions at lower pressure ($Kn>>1$). A more complex behavior that is hard to predict appears in the regions between these extremes. References [7] [8]&[9] discuss the physics of gas transport as a function of the Knudsen number.

In Low Pressure Chemical Vapor Deposition (LPCVD) the mean free path between gas molecule collisions is large compared to the characteristic dimensions of trench and as a result the deposition rate at different points in the trench depends on the velocity distribution of molecules and the manner different parts of the trench “shadow” each other. The equations that describe transport in this Knudsen number regime are similar to ones used in radiation heat transfer and are discussed in detail in [1] and [13]. LPCVD is commonly used in industry and very powerful deposition models have been successfully applied to many applications including 2D and 3D features as well as complex gas-surface chemical reaction models.

In Atmospheric Pressure Chemical Vapor Deposition (APCVD) the mean free path is very small compared to trench dimensions and the gas transport is determined by the standard Navier-Stokes flow model and the continuum diffusion model. Standard methods for solving these equations are well known and have been applied to the solution of feature-scale transport modeling for many types of physical problems and gas-surface chemistries [11],[10] and [16].

In this work we are interested in CVD problems that lie between the two aforementioned cases and have Knudsen numbers that are finite and gas transport is only properly described using the Boltzmann Equation. The Boltzmann Equation is a high-dimensional integral-differential equation that can only be solved exactly in a very limited set of special cases. There have been a number of attempts to numerically solve the Boltzmann equation that fall into two broad categories. The first category of methods try to make significant simplifications to the physical processes by making broad assumptions that allow a quick solution of the transport problem. The most notable work in this class is the Simplified Monte Carlo (SMC) technique by Akiyama and co-workers [2] which shows results that seem to be very promising. Unfortunately, this approach and others like it are always limited by the simplifying assumptions that they make and give quite erroneous results when the former are not satisfied. The other category of methods try to solve the full transport model making no simplifying assumptions usually using the Direct Simulation Monte Carlo (DSMC) method ([4] [3] and [12]). DSMC is the fastest currently available method for solving the Boltzmann Equation. It was recently shown to provide accurate solutions of the Boltzmann Equation in the limit of infinitesimal discretization [14]. Unfortunately previous attempts to use DSMC to model the CVD problem have not always given consistent results and suffered from fairly crude surface and chemistry models. In this work we develop a reliable CVD profile growth model based on the DSMC incorporating sophisticated chemistry and surface movement models.

1.3 Thesis Overview

The presentation of our work will be done in tree major parts. In Chapter 2 we describe our methodology for simulating feature scale surface evolution and present the details of the DSMC gas transport model used in our method. We will also detail the method through which we incorporate non-linear chemistry models into DSMC. In Chapter 3 we give a number of examples that verify our methodology by comparing our results against exact solutions and other numerical methods in various flow regimes. In addition, we will present a number of trends that show the behavior of our model over a number of important deposition parameters and compare the trends with previous results. Chapter 4 will be primarily devoted to a detailed discussion of the models used to simulate the surface evolution with a particular emphasis on the Level Set Method. The fifth and last chapter gives a summary of our work and presents possible extensions.

References:

1. Cale, TS, Merchant, TP, Borucki, LJ, Labun, AH; *Topography Simulation for The Virtual Wafer Fab*. Thin Solid Films v. 365 152-175 2000.
2. Akiyama, Y, Matsumura, S, and Imaishi, N; *Shape of Film Grown on Microsize Trenches and Holes by Chemical Vapor Deposition: 3-Dimensional Monte Carlo Simulation.* J. App. Phys. V. 34 No. 11 1 1995.
3. Coronell DG; *Simulation and Analysis of Rarefied Gas Flows in Chemical Vapor Deposition Processes.* PhD Dissertation MIT 1993.
4. Cooke, MJ and Harris, G; *Monte Carlo Simulation of Thin-Film deposition in a Rectangular Groove.* J. Vac. Sci. Technol. A V. 7 No. 6. Nov/Dec 1989.
5. Bunshah RF (Editor); *Handbook of Thin Film Deposition (Chapter5: Feature Scale Modeling Vivek Singh). 2nd Ed.*, 2002.
6. http://www.batnet.com/enigmatics/semiconductor_processing/CVD_Fundamentals/Fundamentals_of_CVD.html
7. Bird, GA; *Molecular Gas Dynamics and the Direct Simulation of Gas Flows*. Oxford University Press 1998.
8. Vincenti, W and Kruger C; *Introduction to Physical Gas Dynamics*. John Wiley and Sons, Inc. 1965.
9. Hirschfelder, JO, Curtiss, CF, Bird, RB; *Molecular Theory of Gases and Liquids.* John Wiley & Sons, Inc. 1964.
10. Liao, H and Cale, T; *Low-Knudsen-Number Transport and Deposition*. J. Vac. Sci. Technol. A V. 12 No. 4, July/Aug 1994.
11. Pyka, W, Fleischmann, P, Haindl, B, Selberherr, S; *Three-Dimensional Simulation of HPCVD—Linking Continuum Transport and Reaction Kinetics with Topography Simulation.* IEEE Trans. On Computer-aided Dsg. of IC and Sys. V. 18 No. 12 1999.
12. Ikegawa, M and Kobayashi, J; *Development of a Rarefied Gas Flow Simulator Using the Direct-Simulation Monte Carlo Method.* JSME International Journal Series II, V. 33, No. 3, 1990.

13. IslamRaja, M, Cappelli, M, McVittie, J, Saraswat, K; *A 3-dimensional Model for Low-Pressure Chemical Vapor Deposition Step Coverage in Trenches and Circular Vias.* Appl. Phys. V. No. 11 70 1 December 1991.
14. Wagner, W; *A Convergence Proof for Bird Direct Simulation Monte Carlo Method for the Boltzmann Equation.* Journal of Statistical Physics V. 66 No. 3-4 1011-1044 Feb 1992.
15. *Pricnciples of CVD.* Dobkin DM and Zuraw MK. Kluwer Academic Publishers, Dordrecht. April 2003.
16. Thiart, J and Hlavacek, V; *Numerical Solution of Free-Boundary Problems: Calculations of Interface Evolution During CVD Growth.* Journal of Comp. Phys. V. 125 262-276 1996.

CHAPTER 2: METHODOLOGY

The goal of this chapter is to present our methodology for simulating chemical vapor deposition in small scale trenches using the DSMC. This chapter will start with an overview of the methodology outlining the major steps in the simulation process along with how they fit with each other. The rest of this chapter will be dedicated to explaining the details of two key parts of our methodology, namely, the DSMC model we are using for gas transport and the non-linear chemistry model for surface interaction. The other major part of the methodology, namely the surface evolution model, along with detailed examples, will be presented in Chapter 4.

2.1 Methodology Overview

The basic approach we take here is to develop separate models for the gas transport using DSMC and use the resulting deposition information in a separate surface evolution model. An important assumption we are making here is that the surface profile is stationary in the time scale relevant for transport. Such an assumption has been used in previous deposition models and has so far been shown to be valid in many applications [7]. In our methodology the simulation domain is terminated by boundary conditions imposed by the large reaction vessel which provides a fresh stream of reactants. There have been many attempts at creating integrated reactor/trench-scale models that directly couple the deposition simulation to the reactor volume [6][8][13] though in many cases such models are not necessary and are beyond the scope of this work.

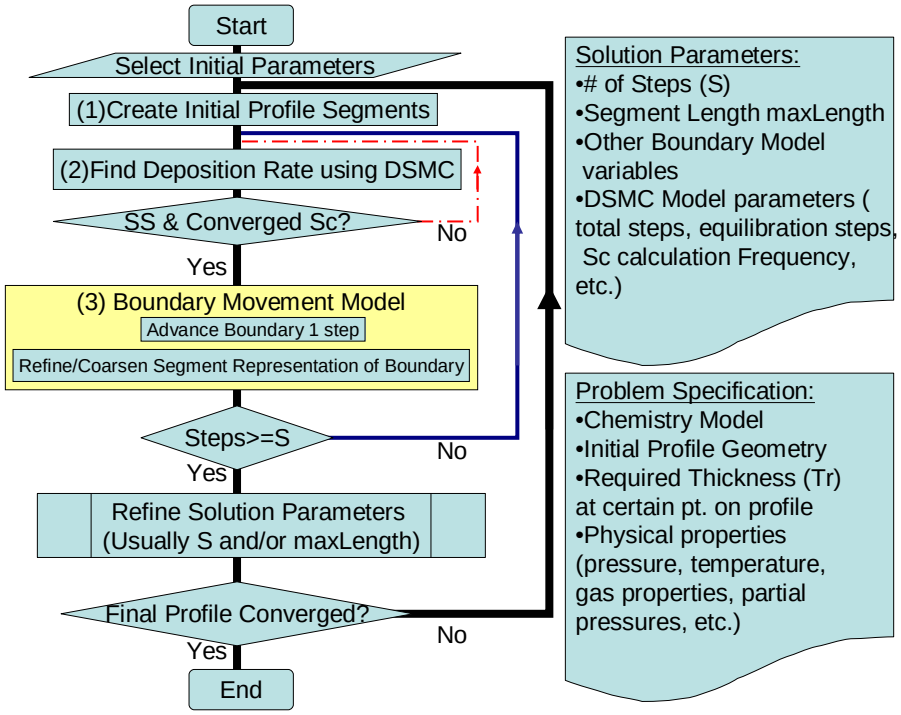

Figure 1: Block diagrams of procedure used in simulating CVD using DSMC with a non-linear chemistry model.

Figure 1 shows a flow diagram of our methodology for calculating the profile resulting from CVD after a finite amount of time t_{final} using S steps. We start by selecting an initial set of parameters that control how refined our profile and DSMC models are. The selection of the proper parameters to give converged results requires some experience and in general the calculation will be repeated with more detailed parameters to ensure the final profile is converged. An initial profile is created based on the problem specifications (Step 1 in Figure 1), which is used as an initial step of our DMSC calculation. The DSMC calculation (Step 2) is run long enough to ensure converged results are reached by meeting two important requirements. The first is that the steady state is reached as judged by the change of the total deposition rate over time. The other requirement is that the chemistry model –if one is used- is converged as will be explained in section 3. The resulting deposition rate is then used by the surface model (Step 3) to create the surface resulting after time= t_{final} /S. The boundary model includes provisions for ensuring the properties of the resulting surface fit within the solution parameters specified at the start (for example the length of all segments<*maxLength* and so on). These steps are repeated

S number of times until the surface profile at end of time t_{final} is found. The whole process can be repeated with more refined parameters to confirm the convergence of the final deposition profile.

2.2 DSMC Gas Transport and Deposition Model

As mentioned before, the Direct Simulation Monte Carlo method is used in this work to account for the gas transport in our CVD trench model. DSMC was invented by Bird [1] in the 1960's as a method of numerically solving the Boltzmann Equation for a wide variety of conditions. The DSMC method is fairly well documented (See [1],[9],[10],[11],[12]&[13]) and so the next sections will only discuss aspects of our implementation that are special or non-standard.

Although the particle dynamics in DSMC are three dimensional, this thesis considers infinite trenches for which a two-dimensional model is sufficient. Nothing fundamentally limits the applicability of our work to 2D problems, although in 3D there may be some complications with our boundary movement model and of course , the computation cost will increase. In Chapter 5 we discuss to possible ways for extending our methodology to handle these cases.

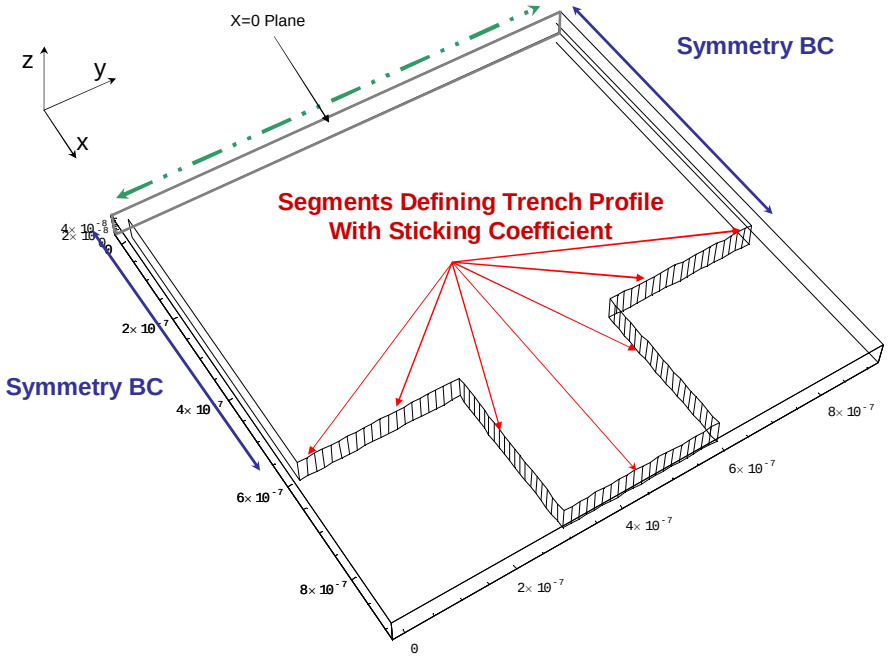

Figure 2: Plot showing the segments of a deposition profile and two different boundary conditions of the DSMC domain. A cyclic (periodic) boundary condition is also applied in the Z-Direction to simulate the effect of an infinite trench.

Figure 2 shows a sketch of the domain and boundaries of a typical DSMC run used in our methodology. The domain is divided into a uniform 2D array of square cells of side lengths of ⅓ the mean free path (λ). The trench segments are free to move in the domain across any of the cells and to ensure that the cell collisions are processed properly, the volume of all cells is calculated using a simple Monte Carlo integration technique at the start of every DSMC step. The domain height in the z-direction is also set to roughly ⅓ λ and a cyclic boundary condition is applied in that direction to simulate an infinitely long trench. The length of the cell along the z-direction is not important because this is fundamentally a 2D problem and in fact we could have totally ignored the positions and movement along this axis to save on computational resources with no effect on the results. Finally, our implementation is set up so that the gas particles in the domain can be divided into an arbitrary number of species that can be independently tracked at all times.

The gas enters the simulation domain through the open wall boundary condition that is applied at the x=0 plane. Particles that cross this boundary and leave the domain of interest are deleted. This boundary condition essentially matches the simulation to an

infinite reservoir (x<0) of specified number density, composition and overall average velocity. Incoming particles are created by filling a larger region (between 0 and -4 λ) with particles with random initial positions and a Maxwell-Boltzmann velocity distribution every time step. The movement of these particles is tracked and the ones that drift into the DSMC domain are kept while retaining their velocity and new position. Although this is more complex than simply creating the particles at x=0 with a biased Boltzmann velocity distribution, it is done to ensure that the particles created not only have the correct distributions for position and velocity but also maintain the correct correlation between these two variables.

The other set of boundaries are created by the trench (shown in red in Figure 2) and the symmetry segments at the ends of the domain (shown in blue). Gas particles in the domain are moved using the standard advection schemes used in DSMC. Collisions with the domain boundaries are also similar in spirit although the arbitrary deposition shape requires the discretization of the latter in a larger number as small linear segments. As the number of boundary segments grows large (in a typical trench there are 50-200 segments) the computational cost of the particle advection step is increased by the same degree. This can have a very significant effect on the speed of our transport model, particularly when we have a large number of segments and/or a low Knudsen number. As will be explained in Chapter 4, there is a simple optimization that can be made to dramatically improve the speed while making no compromises in particle movement accuracy.

Symmetry boundary conditions can be simply applied by specularly reflecting gas particles that collide with the symmetry boundaries. In contrast, the treatment of particles that collide with the growth surface involves the absorption of particles with a certain predefined probability (called the *Sticking Coefficient*); the remainder are diffusely reflected back into the domain. In our calculations both the reactor and the trench are held at the same temperature though it is easy to have different temperature distributions or even non-Maxwell-Boltzmann velocity distributions inside the reactor domain (x<0).

In DSMC, temperature, average velocity and number density of all cells and all species

are defined as statistical averages over small regions of space. In addition, statistics are collected for the number of particles that hit each growth surface segment and the number of particles that "stick" to a segment. These are later used to infer the partial pressure of each species as well as the deposition rate at each segment.

2.3 Deposition Surface Chemistry Models

The emphasis in this work is to study CVD in features due to chemistry that is dominated by gas-surface interaction. There are methods to incorporate gas-gas chemistry in DSMC models ([1] and [2] for example) though it seems that their effect is not always important in feature transport models [5]. More details will follow in Chapter 3 but as a general trend lower sticking coefficients (i.e. particles needing more collisions with the wall before they stick to it) result in better quality profiles while higher sticking coefficients cause the formation of voids and cracks. Traditionally, the sticking coefficient is taken to be a constant that does not change along the trench length or as the trench changes shape due to deposition. Usually "curve fitting" is used to match a constant sticking coefficient with the profiles measured from experimental SEMs and despite its crudeness this method is very successful in producing good estimates of sticking coefficients for many conditions [3].

A number of successful attempts have been made to incorporate more sophisticated models for the calculation of the surface sticking coefficients in both CVD [5] and physical vapor deposition [6]. Our method for calculating Sticking coefficients based on chemistry models for CVD is similar to the method available in the literature though it has been modified to be used within our DSMC framework.

To understand how the sticking coefficient is calculated, assume that there are two gases in our domain that react according to the following formula:

$$A+\beta B \rightarrow \gamma C(s) + \delta D \qquad (1)$$

Here:

β is the number of moles of species B that react with each mole of species A.

and likewise,

γ is the number of moles of species C deposited for each mole of species A that reacts.

δ is the number of moles of species D returning into the gas from the surface for each mole of species A that reacts.

Furthermore, assume that an analytical formula is available for the reaction rate of reaction 1:

$$\text{Rate}=\text{Rate}_A = f[T, pp_A, pp_B, pp_D, \ldots] \qquad (2)$$

where pp_j is the partial pressure of species j.

We proceed by "splitting" the reaction equation into two equations that involve only one of the reactants, for example:

$$A \rightarrow \tfrac{1}{2}\,\gamma\, C(s) + \tfrac{1}{2}\,\delta\, D \qquad (1a)$$

and

$$B \rightarrow \tfrac{1}{2}\,\gamma/\beta\, C(s) + \tfrac{1}{2}\,\delta/\beta\, D \qquad (1b)$$

The partial pressures used in (2) can be inferred from the average number of particles that intersect each segment by the following method [4]. We first try to find the number density starting from the analytical formula for the flux of particles from a gas at equilibrium:

$$\text{Flux} = \frac{n}{4}\bar{c} \quad \Rightarrow n = \frac{4\,\text{Flux}}{\bar{c}}$$

We then proceed to use the ideal gas law to relate the flux of incoming particles to the partial pressure of an equilibrium gas:

$$pp = nmRT \quad \Rightarrow \; pp = 4\frac{\text{Flux}}{\bar{c}}\,mRT \qquad \textbf{(3)}$$

We finally calculate the particle flux into a segment by dividing the effective number of particles that hit the segment by the length of the run and the area of the segment. The implied partial pressure is then used in (2) to find the local rate of reaction at the segment. With the reaction rate at hand the sticking coefficient of species j and for segment i can be calculated from the reaction rate[1] of the species at that segment as follows:

$$Sc(j,i)=Rate_j(i)/Flux_j(i) \qquad \textbf{(4)}$$

Moreover, the number of moles of species C that is deposited is tracked by adding $\gamma/2$ to its counter each time species A is absorbed and $\frac{1}{2}\gamma/\beta$ each time species B is absorbed.

It is important to realize that the way the reaction equation (1) is split to (1a) and (1b) is generally not important as long as the correct ratios for sticking coefficients and reaction rates are recovered in the limit of large number of reacting molecules colliding with the surface. The rationale is that equation (1) is a simplification that only agrees with the real reaction mechanism in an average sense and does not include the details of the real reaction. In a similar manner, it is important that DSMC reproduces the gross chemical behavior in an average sense and not necessarily during every collision.

There are two ways of calculating the deposition flux rate at each section. The first is to directly record the total number of particles absorbed on each segment and convert that to a deposition flux rate. The second method is to use the reaction rate form (2) to calculate the deposition rate at each point (in this example Deposition Rate $=Rate_A*\gamma$). Although these two methods are equivalent in principle, the results of the later are much less noisy when a significant number of particles that hit the wall do not react with it.

The final issue that has to be addressed is the creation of byproduct species that can be important in finite Knudsen numbers. The byproduct species is created after every collision according to its molar ratio to the reacting species in the split chemical formula. For example, in Reaction (1a) $\frac{1}{2}\delta$ particles of species D are created every time species A is adsorbed and likewise $\frac{1}{2}\delta/\beta$ particles of D are created each time Species B reacts with

[1] Actually the reaction that should be used is Min[Rate, $Flux_A$, $Flux_B$] to ensure that the depletion of one species limits the rate of the total reaction.

a segment. The new species are introduced in the domain at the point that the reacting particle hits the surface and they are moved for the balance of the time step duration after the original particle reached the segment. One complicating issue arises when the number of byproduct particles to be created is not an integer and can be dealt with in one of two ways. One way is to split the original reaction equation such that an integer number of byproduct particle has to be created every time a reaction happens. The other solution that is more general is to create an extra particle with a probability equal to the fractional part of the number of particles.

Finally, there have been a number of bold assumptions made in our approach in calculating the sticking coefficients that are not guaranteed to hold in all cases. The most notable example of this is the assumption of an equilibrium gas distribution that results in (3) that we use above. In spite of this, the method is able to give correct results in many different cases and in particular it has been verified at high Knudsen numbers [5][7] where gas particles are sometimes very far off from the equilibrium velocity distribution. This is probably because the reaction rate (2) is much more a function of the number of molecules that arrive at the surface and their average temperature and not a strong function of the velocity distribution function of these molecules.

References:

1. Bird, GA; *Molecular Gas Dynamics and the Direct Simulation of Gas Flows.* Oxford University Press 1998.
2. Boyd, I, Bose, D and Candler, G; *Monte Carlo Modeling of Nitric Oxide Formation Based on Quasi-classical Trajectory Calculations.* Phys. Fluids V. 9 No. 4 1162-1170 April 1997.
3. Junling, L; *Topography Simulation of Intermetal Dielectric Deposition and Interconnection metal deposition Process.* PhD Dissertation Stanford University March 1996.
4. Cale, T, Gandy, T and Raupp G; *A Fundamental Feature Scale Model for Low Pressure Deposition Process.* J. Vac. Sci. Technol.A V.9 No.3 524 1991.
5. Cale, T, Richards, D and Tang, D; *Opportunities for Materials Modeling in Microelectronics: Programmed Rate Chemical Vapor Deposition.* Journal of Computer-Aided Materials Design, V. 6 283-309 1999.
6. Rodgers, S; *Multiscale Modeling of Chemical Vapor Deposition and Plasma Etching,* PhD Dissertation MIT February 2000.
7. Cale T and Mahadev V.; *Low Pressure Deposition Processes.* Thin Films V. 22 172-271 1996.
8. Coronell DG; *Simulation and Analysis of Rarefied Gas Flows in Chemical Vapor Deposition Processes.* PhD Dissertation MIT 1993.
9. Alexander, F and Garcia, A; *The Direct Simulation Monte Carlo.* Comp. In Phys. V.11 No. 6 588-593 1997.
10. Garcia, AL; *Numerical Methods for Physics (2nd Ed.).* Prentice Hall 2000.
11. Bird, GA; *Recent Advances and Current Challenges for DSMC.* Computers Math. Applic. V. 35 No. 1/2 1-14 1998.
12. Oran, E, Oh, C, Cybyk, B; *Direct Simulation Monte Carlo: Recent Advances and Applications.* Annu Ref. Fluid Mech. V.3 403-41 1998.
13. Hudson, Mary, Bartel, Timothy; *Direct Simulation Monte Carlo Computation of Reactor-Feature Scale Flows.* J. Vac. Sci. Technol., A, V. 15 No. 3,1 559-563 1997.

CHAPTER 3: VERIFICATION

The goal of this chapter is to demonstrate that our CVD modeling methodology is in agreement with already existing results that are exact, published or experimentally verified. We will start by describing a number of important definitions that will be useful when analyzing results presented in this and other chapters. The results will be grouped and presented in three different sections based on the Knudsen number and the surface chemistry model. The first section will discuss results of depositions at very low pressures ($Kn \rightarrow \infty$) and with a constant surface sticking coefficient. The second section will describe deposition results which are in the same Knudsen regime but with a non-linear chemistry model which predicts the surface sticking coefficients. We will finally turn our attention to verification problems at high pressure ($Kn \rightarrow 0$) by comparing our results with results from a continuum diffusion model. In addition, trends of key parameters will be presented in an attempt to give a feel for the effect of varying the Knudsen number.

3.1 Definitions of Key Terms

Clear definitions of key ideas and terms are needed before proceeding to present the results. The definitions of the terms used here are similar to the ones used in the literature (see for example [10]) with only some minor modifications or variations. Figure 1 shows a sketch of a typical deposition problem along with dimensions of key importance.

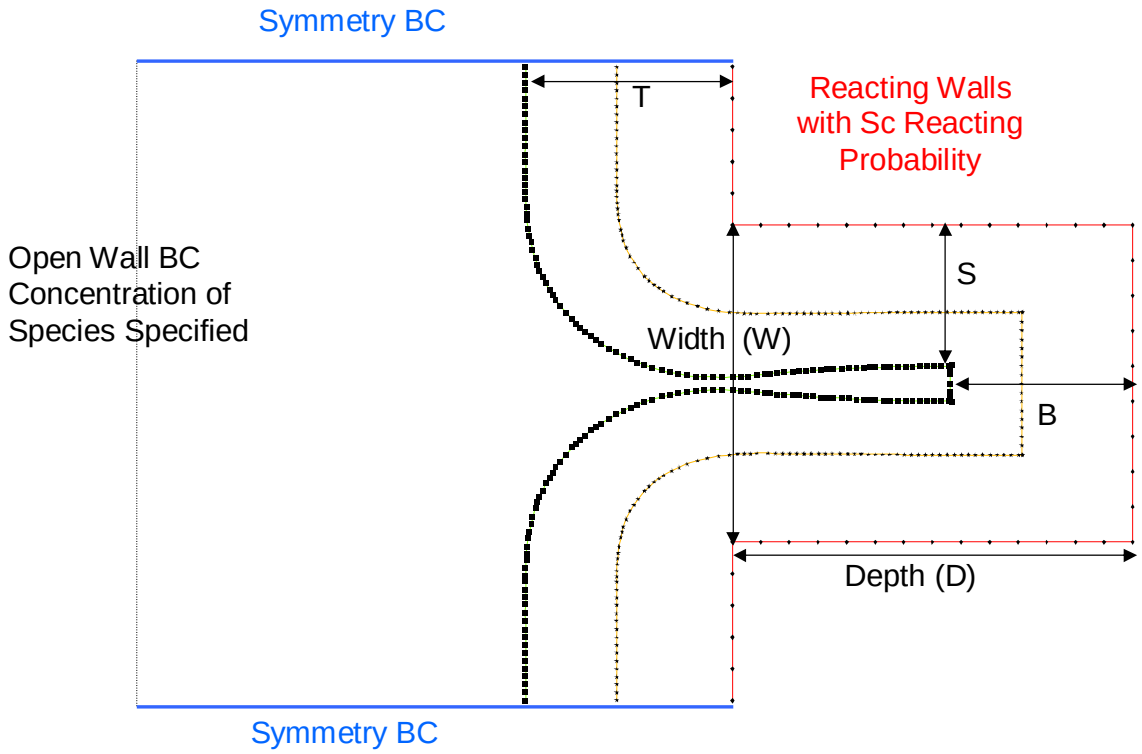

Figure 1: Sketch of basic trench showing important dimensions used to define commonly used terminology.

The *Aspect Ratio* (AR) is the ratio of the width of the trench (W) to the Depth (D) for the deposition profile in the initial state. As the CVD proceeds, different parts of the profile advance at different rates and the emerging profile is described by a number of different measures. The *Corner Step Coverage* (CSC) is the ratio of the side length of the thinnest part in the bottom of the trench (S) to the thickness at the top (T). The *Bottom Step Coverage* (or simply the Step Coverage) is the ratio of the middle of the bottom of the trench (B) to the top thickness T. The *Flux Step Coverage* (FSC) is the step coverage calculated based on the deposition rate at the initial geometry. Deposited profiles that have high step coverages (called *Conformal* profiles) are desirable since they result in profiles that do not develop voids when the deposition is continued until the mouth of the feature is closed.

3.2 Low Pressure Deposition with Constant Sticking Coefficient (Kn→∞)

In this section we start by comparing the accuracy of our code with relation to an exact analytical solution. We then proceed to compare our deposition maps and resulting trench profiles to results from specialized low pressure (Kn→∞) deposition codes that have been independently verified. Next we proceed to compare our new DSMC results to previous attempts at modeling trench deposition for arbitrary Knudsen numbers. As we will see we are generally able to reproduce published results at high Knudsen numbers but have found that we disagree with some of the results for published arbitrary Knudsen numbers.

3.2.1 Comparing LPCVD Results to Analytical Limits and Specialized Programs

The flux step coverage for a trench undergoing LPCVD can be easily calculated analytically in the special case when the sticking coefficient is unity. To see this we start with the trench sketched in Figure 2a that has particles arriving from the left with a cosine velocity distribution. The ratio of the deposited particles at the top of the trench to the midpoint of the bottom of the trench, that is the flux step coverage, is given by [5]:

$$FSC \frac{\int_{-\alpha}^{\alpha} \mathrm{Cos}[\theta]\, d\theta}{\int_{-\pi}^{\pi} \mathrm{Cos}[\theta]\, d\theta}, \qquad \text{with } \alpha = \mathrm{ArcTan}\left[\frac{1}{2\,AR}\right] \Rightarrow FSC = \frac{1}{\sqrt{1+4\,AR^2}} \qquad (1)$$

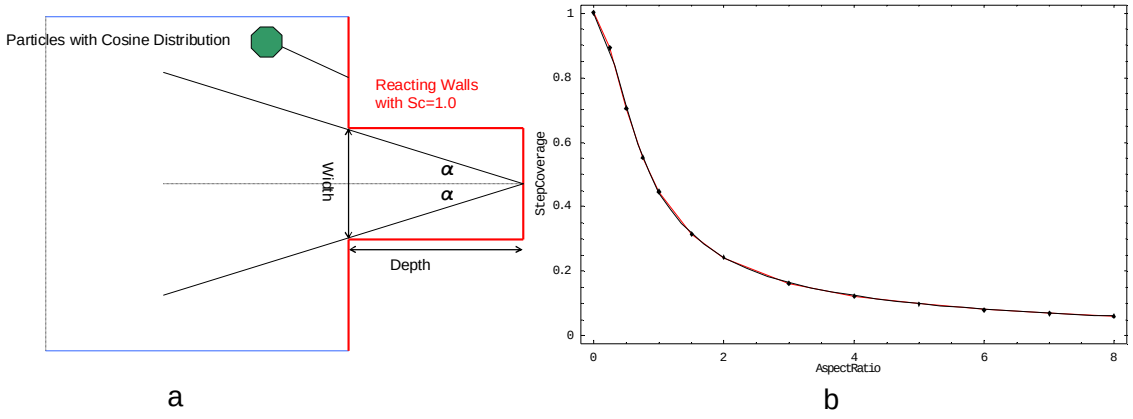

Figure 1: (a) Sketch of trench with a sticking coefficient=1. All particles that come from the left are absorbed at the surface. (b) A plot of the step coverage for different aspect ratios. Points are DSMC results while the solid line is the prediction of the analytical formula.

Figure 2b shows a plot of the analytical formula along with the DSMC results for trenches with aspect ratios ranging from 0 to 8. Clearly there is excellent agreement between the DSMC and analytical results with differences only due to statistical noise.

Unfortunately, the above simple analytical model cannot be extended to cases with Sc<1 or for geometries that are more complex than a simple trench. The problem of solving for the transport at the radiation limit is however very well understood and much advanced work has been done in this field [3][2]. One implementation of this work that has been extensively tested in simple and complex cases is a profile simulator known as EVOLVE developed by Cale and co-workers[7].

Figure 3 shows a sketch of a moderately complex trench (in red) with particles coming in from the left with a cosine (equilibrium) velocity distribution. The results for the deposition profile along the trench length are plotted for both EVOLVE (3b) and DSMC (3b) for two separate sticking coefficients. The agreement between the two codes is almost perfect implying that our particle tracking methods in complex geometries are indeed accurate.

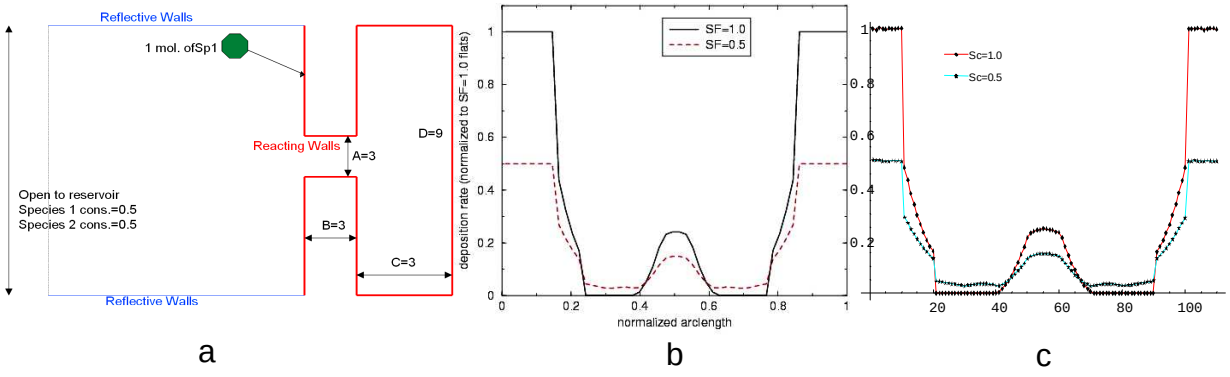

Figure 3: (a) Sketch of complex trench. (b) EVOLVE result for both 1.0 and 0.5 sticking coefficient. (c) DSMC results for the same sticking coefficients.

We now proceed to look at an even more complex example with multiple species and an asymmetric trench (Figure 4). In this example we have low pressure gas with 3 species each with a unique initial flux rate and sticking coefficient at the surface. Species 1 and 2

come in at similar proportions from the left while species 3 is only created as a byproduct of the deposition of Species 1 at the wall as follows:

Sp1 → 3 Sp3 + Deposition @ wall (Sc[Sp1]=0.5)

Sp2 Does not react

Sp3 → no byproduct + Deposition @ wall (Sc[Sp3]=1.0)

As can be clearly seen from Figure 4 the agreement between DSMC and EVOLVE is exceptionally good for all species. It is interesting to note how there is no deposition of Species 3 in the trench areas facing the left since no particles of that species come in from the boundary on the left and there are no gas-gas collisions to return particles back to the surface.

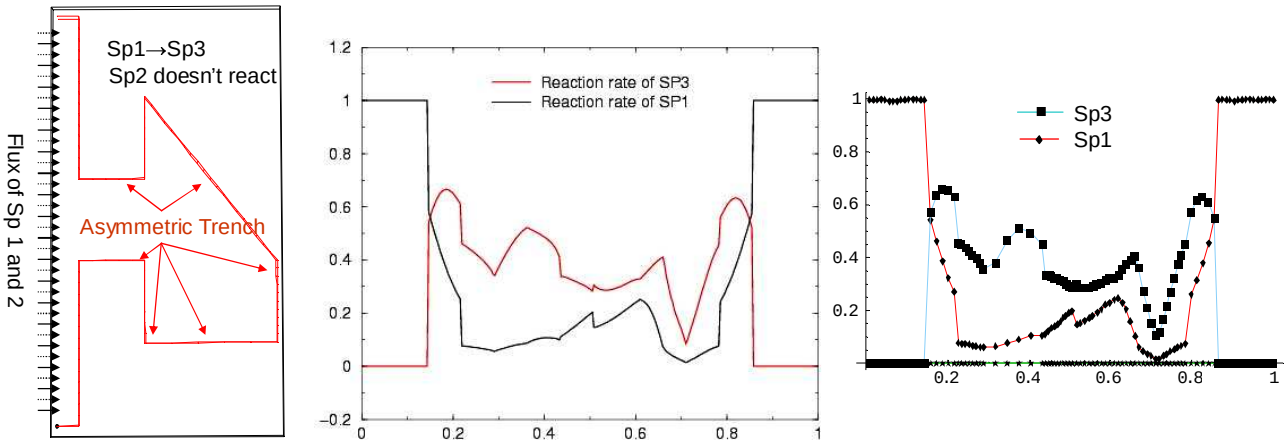

Figure 4: Complex profile, EVOLVE Result and DSMC Result Respectively. The normalization is using the deposition rate of Sp1 on the part of the trench facing left.

Our next example compares results for actual deposition profile evolution based on the flux data from DSMC. Chapter 4 gives more details on how we model and incorporate deposition rate data into profile evolution. The example is of a trench of unity aspect ratio and a constant sticking coefficient of 0.35. Figure 5 shows the result of our calculation (light color) along with published results calculated by SPEEDIE (an other LPCVD deposition software) [2]. The agreement is very reasonable particularly since the Simple Node Tracking method was used with only 20 calls to the DSMC program. Chapter 4

contains an other LPCVD example with a constant sticking coefficient in which DSMC results are compared to EVOLVE profiles.

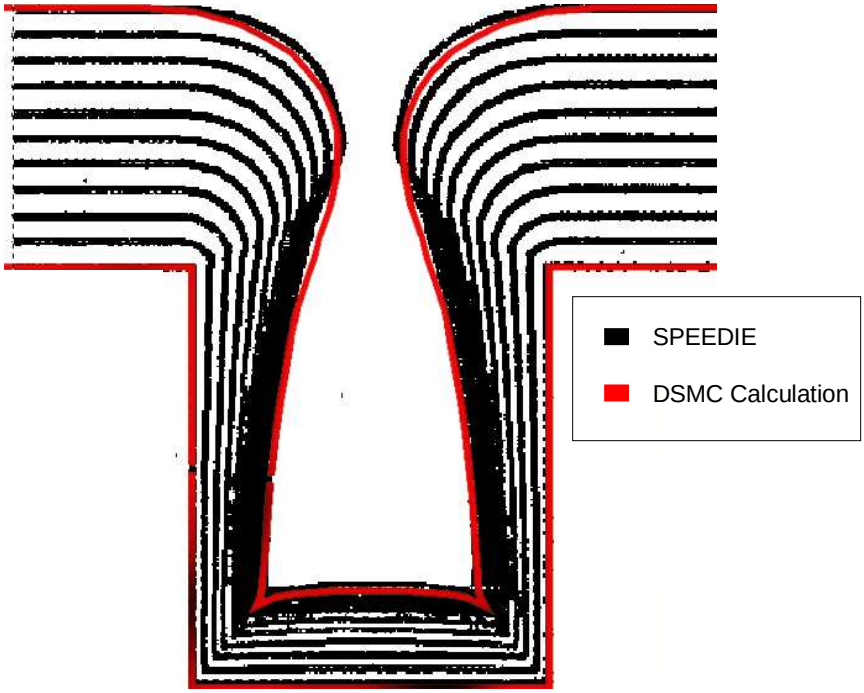

Figure5: Deposition profile results for trench with aspect ratio=1.25 and a sticking coefficient=0.35. Dark lines are for SPEEDIE while light ones are for our DSMC methodology using a simple node tracking surface model.

3.2.2 Step Coverage Trends Calculated for Low Pressure Deposition with Constant Sticking Coefficients

Now that we have established the reliability of our approach in predicting the deposition profiles, we will present a few plots that summarize the profile behavior at different sticking coefficients. Furthermore, we compare our results with those obtained with various other CVD methods designed for the transition regime (~ 0.05<Kn<10). The first plot (Figure 6) is of the corner step coverage in a unity aspect ratio trench as a function of the sticking coefficient. The step coverage is calculated at the point when the thickness of the deposition layer is half the width of the feature and in all cases the profile is calculated using 10 calls to the DSMC program. The red line in the same figure shows

the results published in [4] of the same set of cases calculated using a different DSMC-based method. The agreement between the two trends is very reasonable and the difference is probably mainly due to the variations of profile moving model.

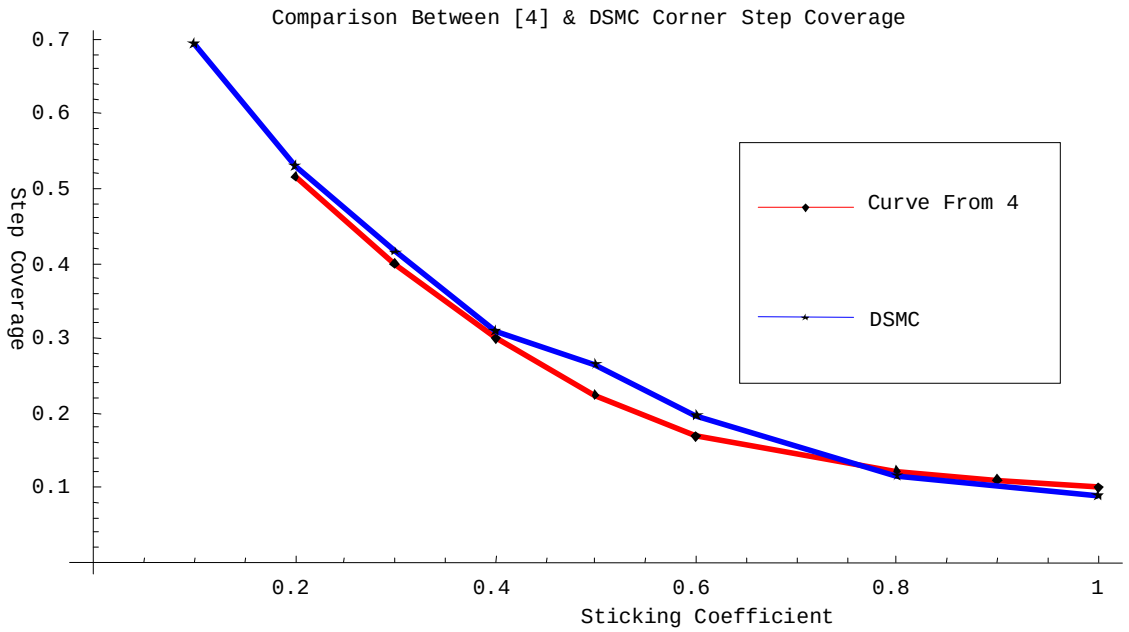

Figure 6: Step coverage versus sticking coefficients of trenches with AR=1 at a deposition thickness=½ width of feature and Kn=∞. Plot compares our DSMC results with those published in [4].

A different parameter (the bottom step coverage) is plotted in Figure 7 for the same set of cases. Again the two red and blue curves are for the step coverages calculated at a thickness of ½*width of the initial trench similar to Figure 6. Upon examination it is clear that the results in [4] do not agree with our calculations even when the solution parameters are varied.

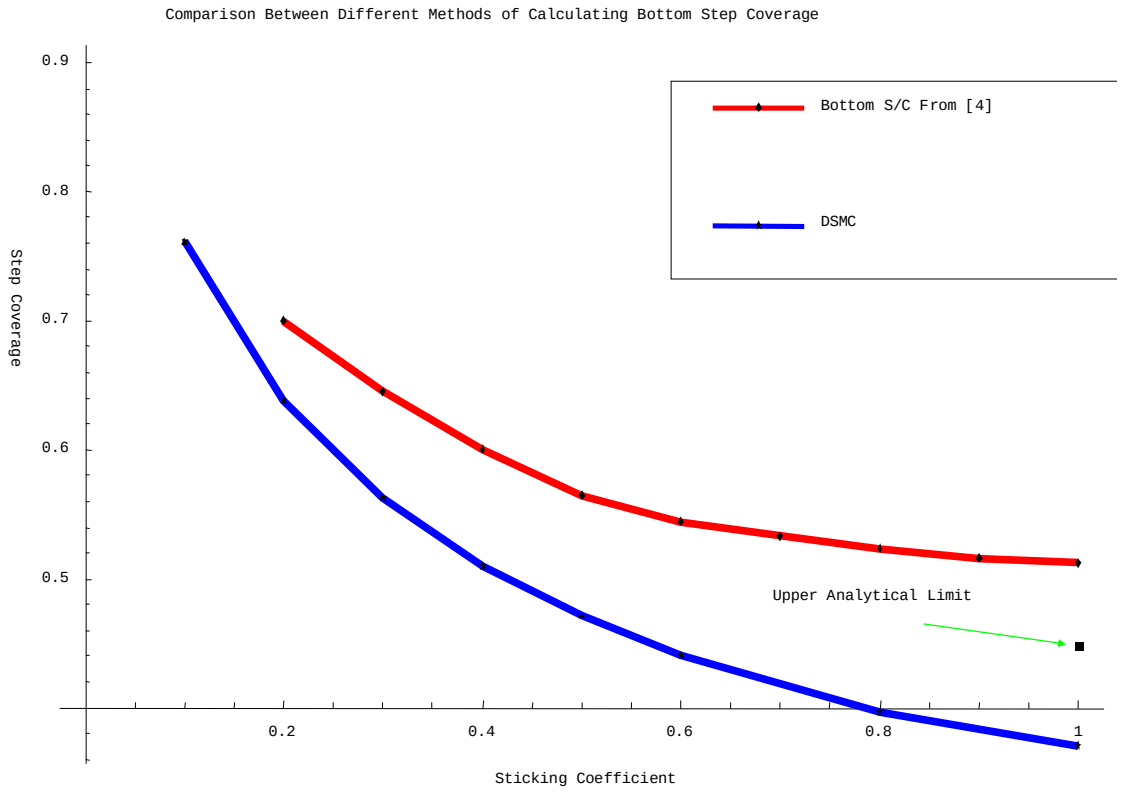

Figure 7: Results for step coverage versus the sticking coefficient for a AR=1 trench at Kn=∞. The red curve is result reported in [4] while blue curve is our DSMC calculation. In both cases the step coverage is calculated at a deposition thickness=½trench width. The analytical result is from equation (1).

A number of clues need to be considered to confirm that our results are indeed the more accurate ones. To begin with, our results agree well with other codes that have been designed and verified in the vacuum limit (namely, EVOLVE [7] and SPEEDIE [2][18]). Also, equation 1 gives us a strict upper limit on the step coverage when the sticking coefficient is 1 because the step coverage decreases with time. The red curve clearly violates this inequality. Finally, the lack of detailed experimental results verifying the trends of [4] also reduces confidence in their accuracy.

3.3 Surface Step Coverage for LPCVD using a Non-Linear Chemistry Model

This section presents our results for the simulation of LPCVD on 2D trenches with a non-linear surface chemistry model and comparing them with published results. Our goal is to verify our methodology and code by reproducing Kn→∞ results where the particle velocity distribution is the furthest away from equilibrium and it is where we expect the greatest deviation if our method does not hold. In what follows we will proceed to explain the chemistry model that will be used in the examples of this section followed by a detailed discussion of our results for a trench on an aspect ratio of 10. We also discuss the convergence of the step coverage. We will then show that our methodology accurately reproduces EVOLVE trends over a wide range of model parameters.

3.3.1 Tungsten Deposition Surface Chemistry Model

We selected the reduction of Tungsten from tungsten hexafluoride as the non-linear gas surface chemical reaction to model in this section. Nothing in our algorithm or implementation is unique to Tungsten and only a change of the chemical species and the reaction rate equation is needed to be able to model other reactions (see [10], [7], [3] or [11] for details of modeling other reactions). Reference [16] gives a detailed discussion of modeling Tungsten chemistry but for this example we will use the simple formula[17]:

$$WF_6 + 3H_2 \rightarrow W(S) + 6HF \qquad \textbf{(1)}$$

and the reaction rate:

$$Rate = 7.16233\, Exp\left[\frac{-8800}{T}\right] \sqrt{pp_{H_2}} \left(\frac{pp_{WF_6}}{pp_{WF_6}^{Ref}} \frac{1 + K_F\, pp_{WF_6}^{Ref}}{1 + K_F\, pp_{WF_6}} \right) \qquad \textbf{(1a)}$$

where:

Rate: is reaction rate/mole of reactants [mol/(s*m^2)]

T: Temperature [K]

pp_{H_2}: Partial Pressure of H_2 [Pascal]

pp_{WF_6}: Partial Pressure of WF_6 [Pascal]

$pp_{WF_6}^{Ref}$: Partial Pressure of WF_6 at entry [Pascal]

K_F: Constant=7.5/Pascal

As explained in Chapter 2 in our model the reaction is actually split up into two reactions that on average reproduce (1) as follows:

$$WF_6 \longrightarrow \frac{1}{2} W(S) + 3HF \qquad \textbf{(2)}$$

and

$$H_2 \longrightarrow \frac{1}{6} W(S) + HF \qquad \textbf{(3)}$$

with a H_2 deposition rate equal to the times the rate defined in (1a).

In our calculation we ignore the creation and the transport of HF. This saves on computing resources and does not affect the results because at high Kn values the lack of collisions means that the increase in HF number density does not reduce the flow of the other species to and from the surface.

3.3.2 Detailed Example of Tungsten LPCVD

The first example of Tungsten deposition will be in a trench with an aspect ratio of 10. The simulation is carried out by taking H_2 with an incoming partial pressure of 4.66 Pascal and WF_6 with a partial pressure of 0.466 Pascal. The surface profile is integrated until a cavity is created when the feature pinches off as can be seen in Figure 8. The simple node tracking model was used to follow the evolution of the profile shape and the step coverage value at closure is predicted within 1% of the published value. The integration of the profile was carried out with only 8 DSMC program calls from start to closure.

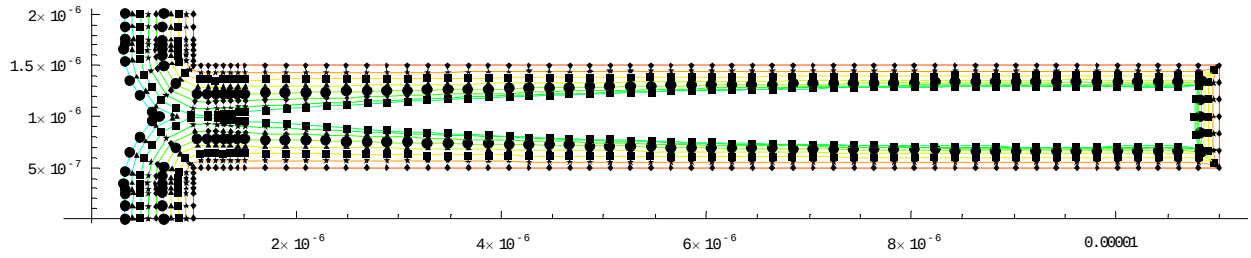

Figure 8: Plot of deposition profile of an AR=10 trench up to closure.

Figure 9 shows a plot of a number of important parameters along the length of the profile for both species as the feature is filled. As the feature fills the partial pressure of WF_6 significantly decreases inside the feature which results in a drop in the deposition rate. Since the partial pressure of H_2 is not significantly reduced, the lower deposition rate results in a lower H_2 sticking coefficient in contrast with the sticking coefficient of WF_6 which increases to a maximum value because 1a is essentially linear at lower WF_6 pressures.

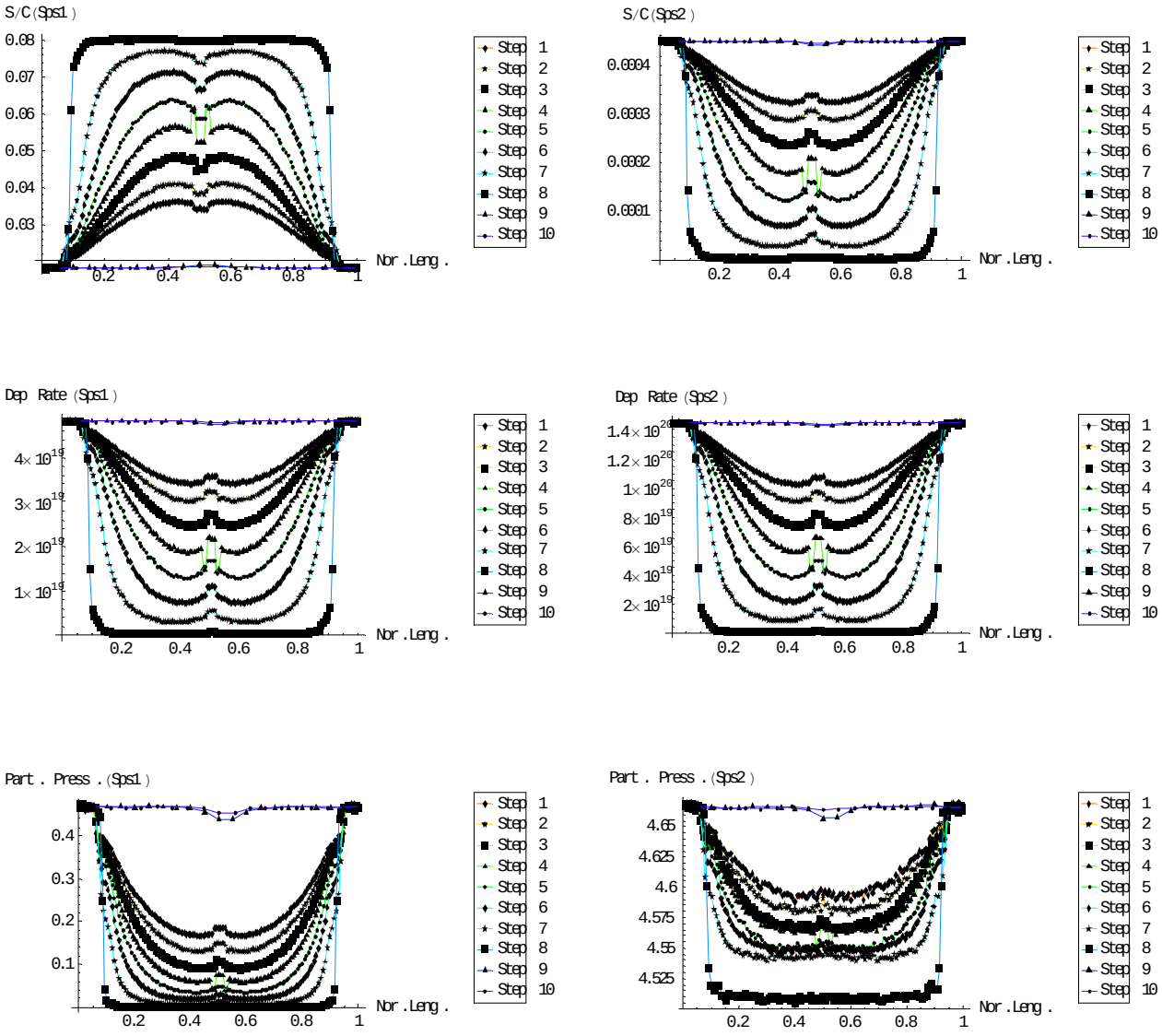

Figure 9: Plot of key parameters versus trench length for the 10 steps that are shown in Figure 8. The left column is for Species 1 (WF_6) and right column is for Species 2 (H_2). Feature is closed after step 8.

Critical to the accuracy of the results presented above is the calculation of the sticking coefficient in a robust manner. An approach that we have found to give reasonable accuracy was to first perform an "equilibration" run with short intervals between Sc re-calculations (details in Chapter 2). We then use the resulting sticking coefficient map as a starting guess for a longer run to confirm convergence. The equilibration here is numerical in nature since at such high Knudsen numbers the problem is almost immediately steady state as far as the transport is concerned. The sticking coefficients are

considered converged when there is no appreciable systematic drift in their values and the only change that happens with time is due to the reduction of noise because of better sampling.

3.3.3 EVOLVE and DSMC Trends

To further validate our methodology, calculations similar to the one detailed in the last section are preformed and compared to results of EVOLVE in [10] and [17]. Figure 11 shows a plot of the corner step coverage at closure of a unity aspect ratio trench at a number of different temperatures with WF_6 and H_2 concentrations identical to those in the last section. DSMC accurately reproduces the EVOLVE trend with the majority of the points only 2-3% away. Figure 12 is a plot of the step coverage at 723K of trenches of various aspect ratios for EVOLVE and our DSMC program. A similar agreement between the two programs can be seen and in fact the agreement on the AR 10 trench is within 0.5%!

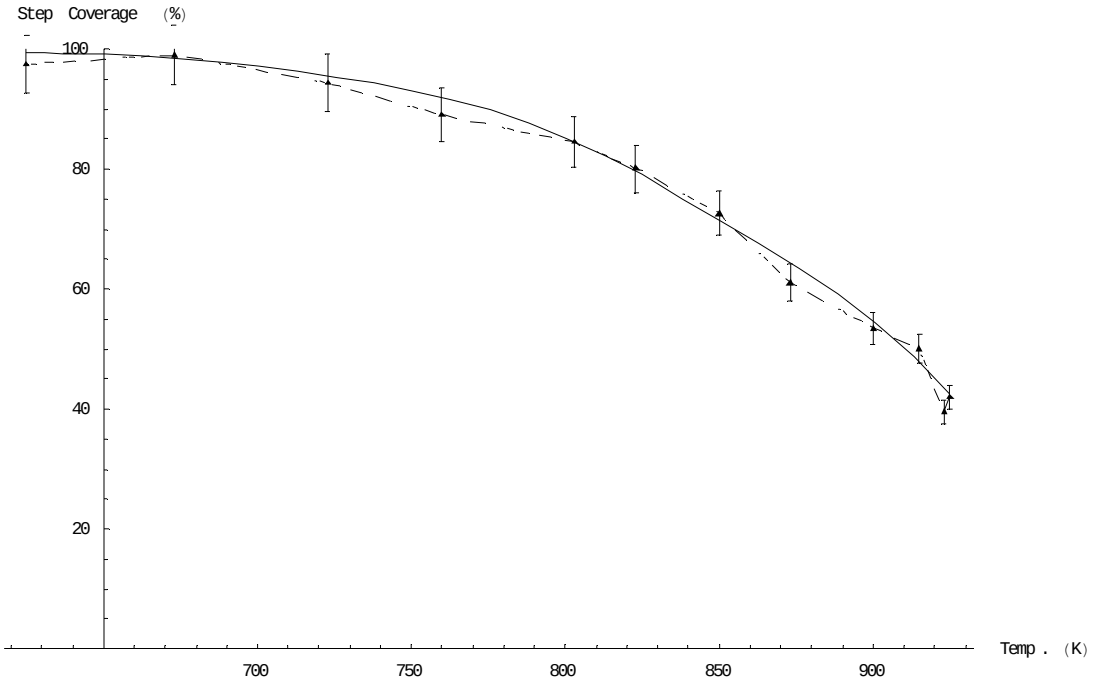

Figure 11: Plot of step coverage vs. temperature for Tungsten CVD on an aspect ratio 1 trench with a pp H_2/ppWF_6=10. The solid line is taken from [10] while the points are DSMC results. Error bars indicate a 5% error margin.

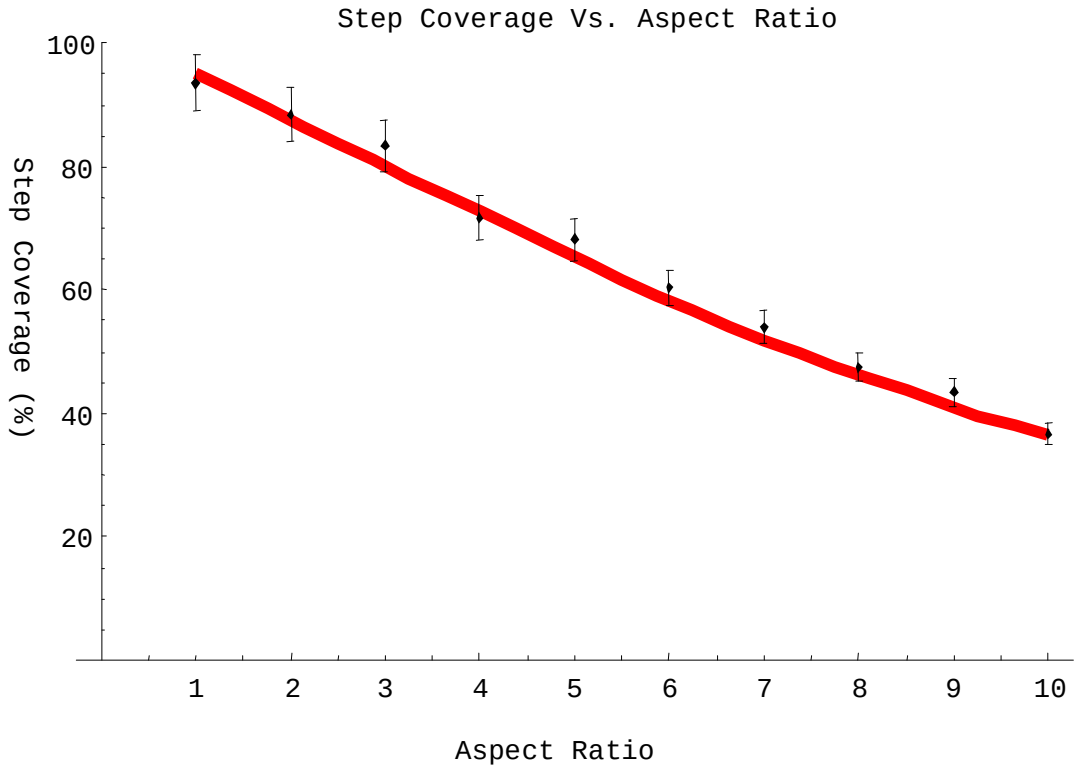

Figure 12: Step coverage values for Tungsten CVD for various aspect ratios at a temperature of 723K and $ppH_2/ppWF_6$=10. The solid line is from [10] while the points are DSMC results with ±5% error bars.

3.4 CVD at High Pressures (Kn→0)

3.4.1 Continuum and DSMC Model Results

Taken together, the results in the last section give us confidence in our methodology for both simple and complex non-linear surface chemistry models in the very low pressure (Kn→∞) regime. In this section we present our DSMC results for high pressure CVD and compare them with results obtained using continuum diffusion finite element analysis (FEA) techniques using a constant sticking coefficient.

A constant sticking coefficient is used here to simplify the continuum equations and their solution. Our DSMC methodology would be identical if we wanted to use a non-linear surface chemistry model. The development of special boundary conditions for the

continuum model with a non-constant Sc on the walls is a bit more involved and is beyond the scope of our work though it is discussed extensively in [8], [9] and [12]. In all of our lower Kn number examples the particles that react with the wall release physically identical but non-sticking particles that are released back into the gas. This is done to ensure that there is no net mass flux into the surface, thus canceling convection terms from the continuum model.

The equation that determines the steady state number density (n_i) of species i is [13]:

$$D_{aa} \nabla^2 n_i = 0$$

D_{aa} is the self diffusion coefficient of our gas and is available from standard gas dynamics theory. For hard spheres its value is [14]:

$$Daa = \frac{3}{8} \frac{\sqrt{\pi m k T}}{\pi d^2 m n}$$

where d is molecule diameter, n is the number density, m is mass and k is the Boltzmann Constant.

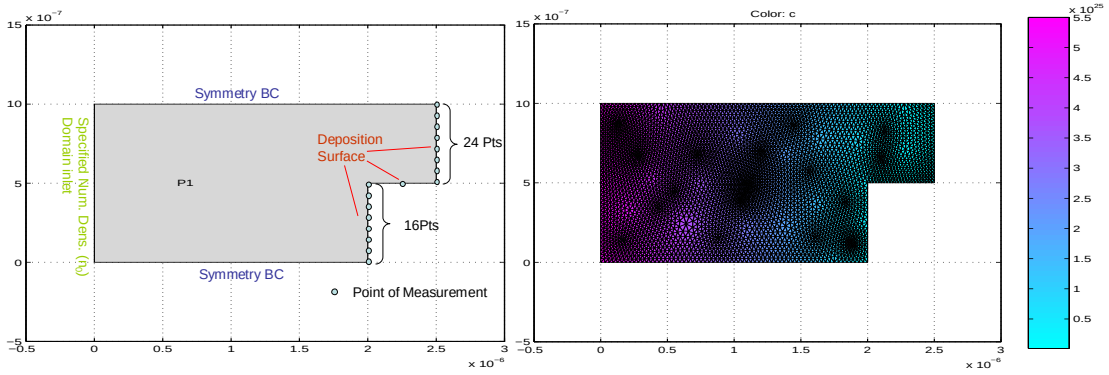

Figure 13: Finite Element Model of the continuum diffusion problem solved to compare with the DSMC calculation results.

Figure 13 shows the meshed solution domain used to solve the problem for a trench with aspect ratio AR=½. A symmetry boundary condition ($dn_i/dy=0$) is used to impose a no mass flux state on the top and bottom edges, while a constant number density n0 is assumed along the left edge to represent the domain inlet. The exact value of the imposed

number density is taken from the DSMC results to account for slip effects and is the only input imported from that model. At the deposition surface the following boundary condition is used:

$$\text{Mass Flux at Trench Edges} = \frac{1}{4} C n = D_{aa} \frac{d n}{d\,\text{normal}}$$

This physically means that at the deposition edge of the domain the particle flux from the domain must be equal to the diffusive flux due to the number density gradient in the domain.

The continuum domain is meshed and solved by using the Pdetool package of MATLAB [15] and the solution is taken to be converged when its values at the deposition edges do not change as the domain mesh is refined. The flux rate along the trench is calculated by the flux formula from equilibrium gas dynamics:

$$\text{Trench Flux} = \frac{1}{4} \bar{C} n_{\text{FE Solution}}$$

where $n_{\text{FE Solution}}$ is taken as the number density value along edge nodes.

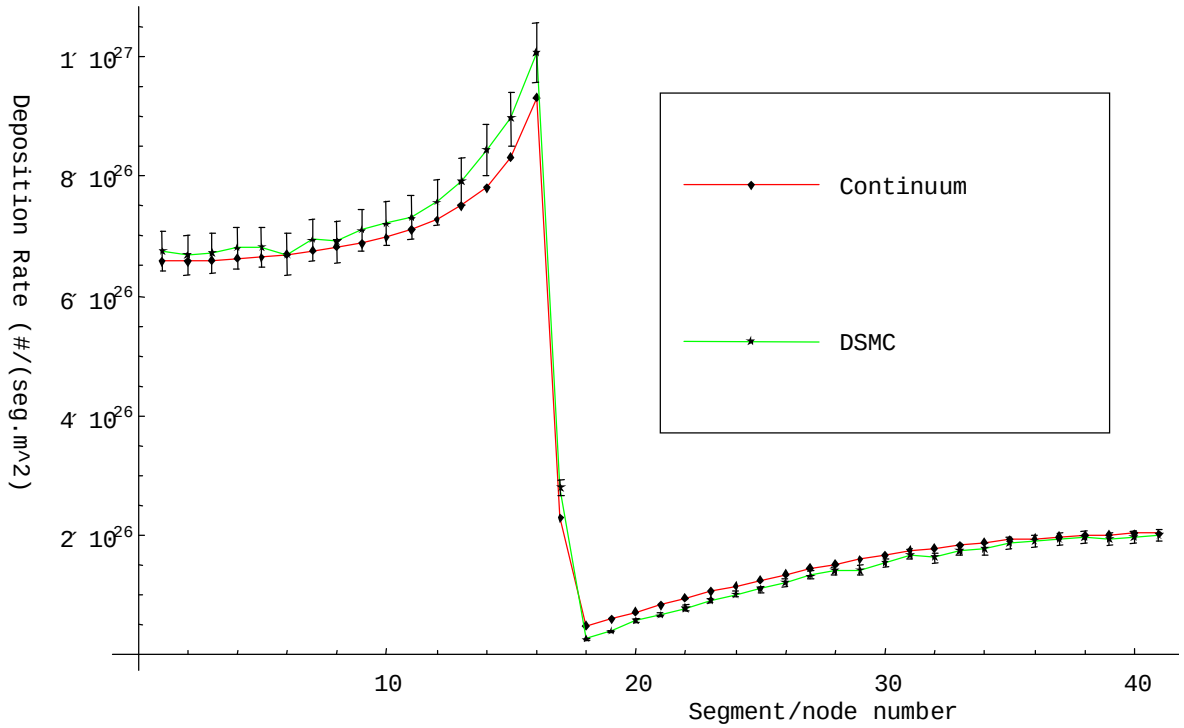

Figure 14: FEM and DSMC results for the deposition rate along the trench at the measurement points sketched in Figure 13. The error bars are ±5% of local value. Problem parameters: Sc=1.0 500,000 particles Kn=0.03 and AR=3.

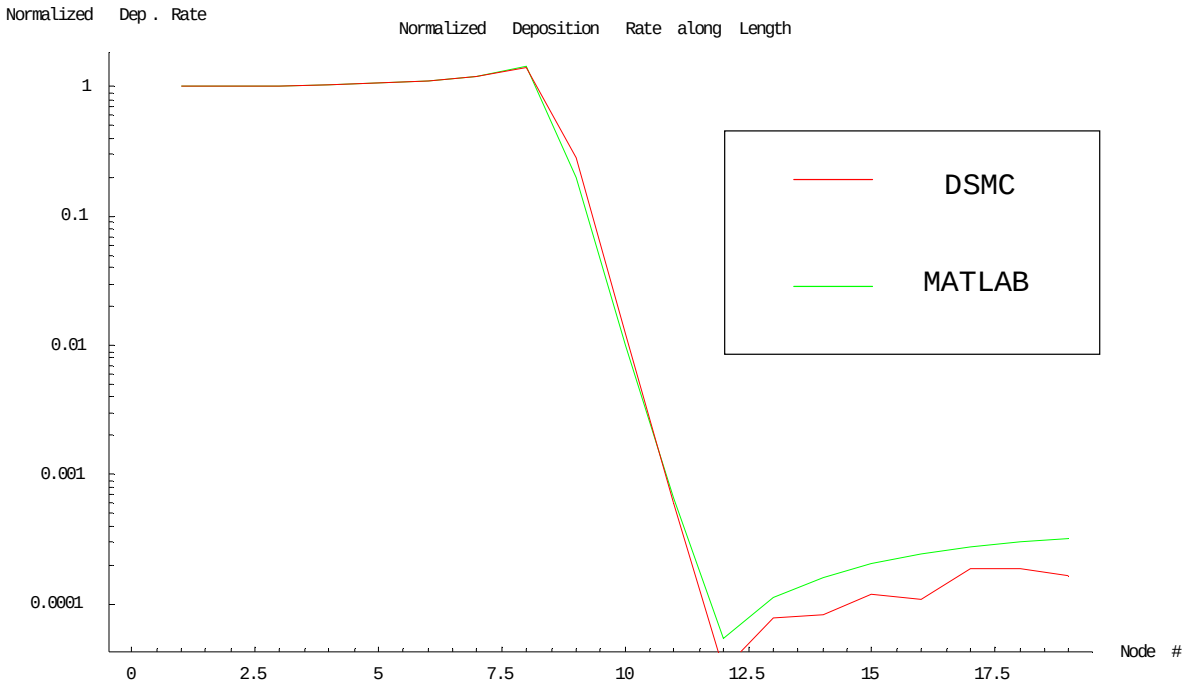

Figure 15: Comparison between the deposition rates as calculated from DSMC and FEA along the length of an AR=3 the trench with a Sc=1.0. We are plotting the natural log of the solution because there is a large change in magnitude between the top and bottom of the trench. The values are normalized to the deposition rate of the node at the top of the solution domain.

Figures 14 and 15 plot the deposition rate of the problem as calculated by DSMC and the continuum problem explained in the last paragraphs. Both calculations were performed using a gas at 300 Kelvin and an appropriate pressure to give a Kn=0.03 on a trench of 1 μm width. For the DSMC calculation care was taken to ensure that steady state was reached before starting to take samples to measure the deposition rate. Figure 14 shows the deposition rates for a ½ aspect ratio trench with error bars ±5% of local value. Clearly, the agreement for both the deposition values along the trench and the inferred flux step coverage is excellent. The same calculations are made for an aspect ratio 3 trench of the same width and gas properties. Figure 15 shows a log linear plot of the deposition rate along the trench normalized to the rate at the axis of symmetry at top of this trench. Again the agreement is very good particularly when one notes the drastic change in the deposition rate value between the top and the bottom of the trench. These test problems, as well as other not presented here, indicate that our DSMC simulation captures gaseous transport for all ranges of Knudsen numbers.

3.4.2 Step Coverage Trends with different Knudsen Numbers

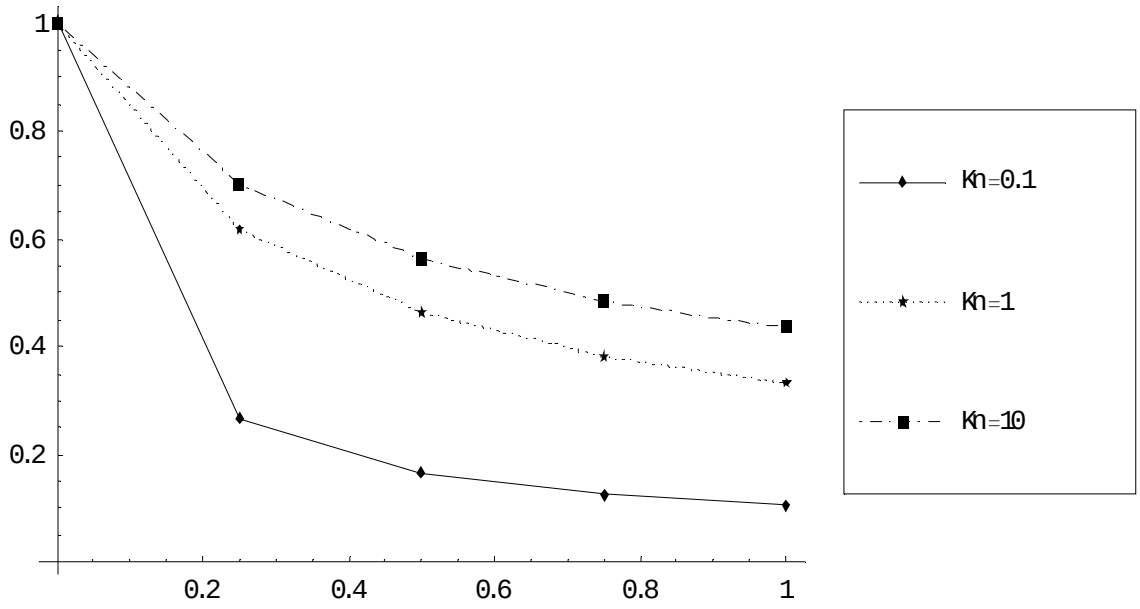

Figure 16: Flux step coverage at base versus Kn and sticking coefficient for an aspect ratio 1 infinitely deep trench. Argon gas was used with a trench width of 1 μm.

A feel for the trends in this class of deposition problems can be gained by examining the plots in Figure 16. The flux step coverage is plotted against sticking coefficients for a number of different Kn values. This set of calculations was carried out using Argon on a unity aspect ratio trench with different pressures to vary Kn. As expected, the step coverage is unity when the sticking coefficient is zero and monotonically decreases with higher sticking coefficients for all values of Kn. There is also a significant decrease in the flux step coverage as the Knudsen number is decreased in all cases. This is in qualitative agreement with the results of Cooke and Harris [1] as well as Kobayashi et el. [4]. The decrease in step coverage is easily explained by the fact that collisions work to "segregate" regions of trench and result in larger differences in number densities and flux rates. Although step coverage at high Kn values does not change with different gases and temperatures it is a function of these and other parameters at lower Knudsen numbers. This is because the diffusion coefficient and hence the transport is a strong function of these parameters which means that no simple universal trends can be created for lower Knudsen number problems.

We finally would like to note that when at low Kn it is important to include enough of the domain above the trench in the model. This is done to ensure there are no concentration gradients across the open wall boundary condition that would cause changes in the deposition rates as a function of area included in the model. In our work we found that a distance of about 1-2 trench widths gave sufficiently accurate results but it must be understood that this may vary significantly with different problem details and only experimentation with different lengths can ensure convergence. A discussion of this issue in the continuum case (where the issue is most significant) can be found in [9].

References:

1. Cooke, MJ and Harris, G; *Monte Carlo Simulation of Thin-Film Deposition in a rectangular Groove.* J. Vac. Sci. Technol. A V.7 No.6. Nov/Dec 1989.
2. IslamRaja MM, Cappelli MA and others; *A 3-Dimensional Model for Low Pressure Chemical-Vapor-Deposition Step Coverage in Trenches and Circular Vias.* J. Appl. Phys. V. 70 No. 11 1 December 1991.
3. Cale, T, Richards, D and Tang, D; *Opportunities for Materials Modeling in Microelectronics: Programmed Rate Chemical Vapor Deposition.* Journal of Computer-Aided Materials Design, V. 6 283-309 1999.
4. Ikegawa, M, Kobayashi, J, Maruko, M; *Study on the Deposition Profile Characteristics in the Micron-scale Trench Using Direct Simulation Monte Carlo Method.* Transaction of the ASME Fluids Engineering Division V. 120, June 1998.
5. Akiyama, Y, Matsumura, S and Imaishi, N; *Shape of Film Grown on Microsize Trenches and Holes by Chemical Vapor Deposition: 3-Dimensional Monte Carlo Simulation.* J. App. Phys. V. 34 No. 11 1 1995.
6. Coronell, DG; *Simulation and Analysis of Rarefied Gas Flows in Chemical Vapor Deposition Processes.* PhD Dissertation MIT 1993.
7. Cale, T and Mahadev, V; *Low-Pressure Deposition Processes,* Thin Films V. 22 1996**.**
8. Liao, H and Cale, TS; *Low-Knudsen-Number Transport and Deposition.* J. Vac. Sci. Technol. A V. 12 No. 4 Jul/Aug 1994.
9. Liao, H; *High Pressure Chemical Vapor Deposition and Thin Film Thermal Flow Process Simulation.* PhD Dissertation Arizona State University 1995.
10. Jain, MK; *Maximization of Step Coverage at High Throughput During Low-Pressure Deposition Process.* PhD Dissertation Arizona State University 1992.
11. Rodgers, S; *Multiscale Modeling of Chemical Vapor Deposition and Plasma Etching.* PhD dissertation MIT 2000.

12. Kleijn, C; *Computational Modeling of Transport Phenomena and Detailed Chemistry in Chemical Vapor Deposition - a Benchmark Solution.* Thin Solid Films V. 365 294-306, 2000.
13. Bird, R, Stewart, W and Lightfoot, E; *Transport Phenomena (3nd Ed.).* John Wiley and Sons 2002.
14. Hirschfelder, JO, Curtiss, CF, Bird, RB; *Molecular Theory of Gases and Liquids.* John Wiley & Sons, Inc. 1964.
15. http://www.mathworks.com/access/helpdesk/help/toolbox/pde/pde.shtml
16. Kleijn, C, Kuijlaars, K Okkerse, M, van Santen, H and van den Akker, H; *Some recent Developments in Chemical Vapor Deposition Process and Equipment Modeling.* J. Phys. IV France V.9 1999.
17. Join M, Cale, T and Gandy, T; *Comparison of LPCVD Film Conformalities Predicted by Ballistic Transport Reaction and Continuum Diffusion Reaction Models.* J. Electrochem. Soc. V. 140 No. 1 January 1993.
18. Rey J, Cheng, LY, McVittie, J and Saraswat, K.; *Monte Carlo Low Pressure Deposition Profile Simulations.* J. Vac. Sci. Technl. A, V. 9 1083 1991.

This page is intentionally left blank.

CHAPTER 4: SURFACE MOVEMENT MODELS

The Level Set (LS) methodology is a very elegant and powerful approach to modeling evolving complex boundaries. The methodology is particularly attractive when dealing with boundaries of arbitrary topologies in three dimensions since it only requires the machinery developed for simple two dimensional cases. In this chapter we will discuss the details of our Level Set formulation of evolving boundaries due to CVD. Furthermore, we will cover the details of a simple 2D method of profile evolution and use it as a benchmark to compare the LS method against. We will finally detail a simple method of improving DSMC code performance based on a basic level set idea.

4.1 Motivation & Background

The accurate prediction of the surface profiles that result from CVD depends on two factors: the ability to accurately find the flux rates at every point at the growing interface and the ability to advance the profile in physically consistent way that properly incorporates the deposition rate data. The first requirement is totally dependent on the transport model that is explained in Chapter 2. The second requirement is a surprisingly subtle subject particularly when dealing with discontinuity of slopes, stability and topology changes common in CVD problems faced in practice [3]. To appreciate this point, take the problem of dealing with the initial curve shown in Figure 1 as an example. The curve has two segments with significantly different deposition rates on each segment. Although it is easy to see how the curve should move with time in the areas that are straight with a constant deposition rate, it is not intuitive which shape the curved segment between them should take. Chapter 5 of [7], [8] and [3] are good starting points for literature that discusses these problems and how one goes about solving them in a manner that faithfully represents the physics that the original boundary and deposition rate represent.

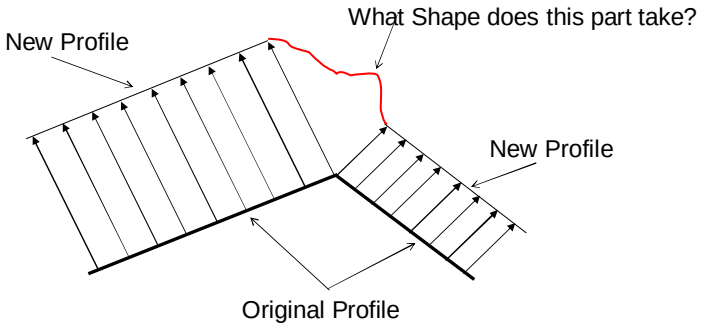

Figure 1: How is the curve defined in the middle section?

Over the years a large number of approaches have been proposed to accurately model interfaces with various degrees of success (Chapter 4 of [7] has a good overview of some of these methods with some advantages, disadvantages and development history). In our work in CVD profile modeling we have developed and used a simple string tracking model as well as a more sophisticated Level Set based profile model that is based on Osher and Sethian's work [9].

4.2 Profile Evolution Models

In what follows we will describe the two profile evolution models that we have used in our work in modeling the boundary evolution due to the deposition predicted by DSMC. The first surface model is a simple node tracking model that works for simple 2D geometries while the second model is based on the Level Set method which is aimed at more complex geometries and surface models. After describing the basic concepts behind each model we will proceed to describe some of the details of implementation of each model and we will conclude with some examples that demonstrate the reliability of both models when used with the appropriate parameters.

4.2.1 Simple Node Tracking

Our goal in developing and using this method is to have a simple reference model to compare our more complex LS implementation to. This simple method is able to produce accurate profile results and was of great help in identifying the different causes of errors

in our Level Set Development. The main limitation of this model is that it can not be easily extended to include more complex surface effects (surface diffusion for example) and that it cannot be readily extended to the treatment of 3D surface evolution.

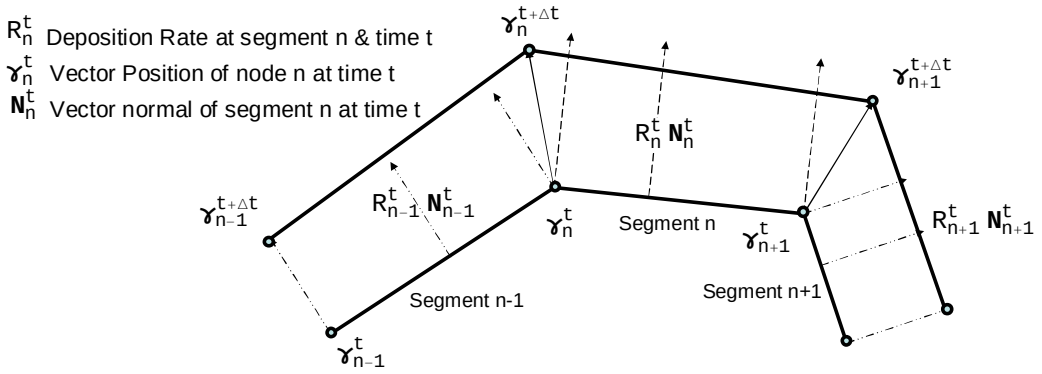

Figure 2: Sketch of simple node tracking. Note how arrows are sometime longer or shorter than the distance the segments move.

The basic steps of the method can be easily explained by referring to Figure 2, which shows one step of the method between times t and t+Δt. The curve is defined by the N-1 segments that extend between the nodes γ_n^t, were n=1,…, N. Node n moves as follows:

$$\Delta\gamma_n^t = \gamma_n^{t+\Delta t} - \gamma_n^t = \frac{1}{2}\left(R_n^t \mathbf{N}_n^t - R_{n-1}^t \mathbf{N}_{n-1}^t\right)$$

where R_n^t and $\mathbf{N}_n^t$ are defined on Figure 2.

In other words, a node moves by a vector distance equal to the average of the normal velocity of the surrounding segments. The end nodes (i.e. Node 1 and N) are dealt with by assuming a symmetry boundary condition which amounts to using the projection of the speed vector of the first and last segment in the direction parallel to the symmetry boundary.

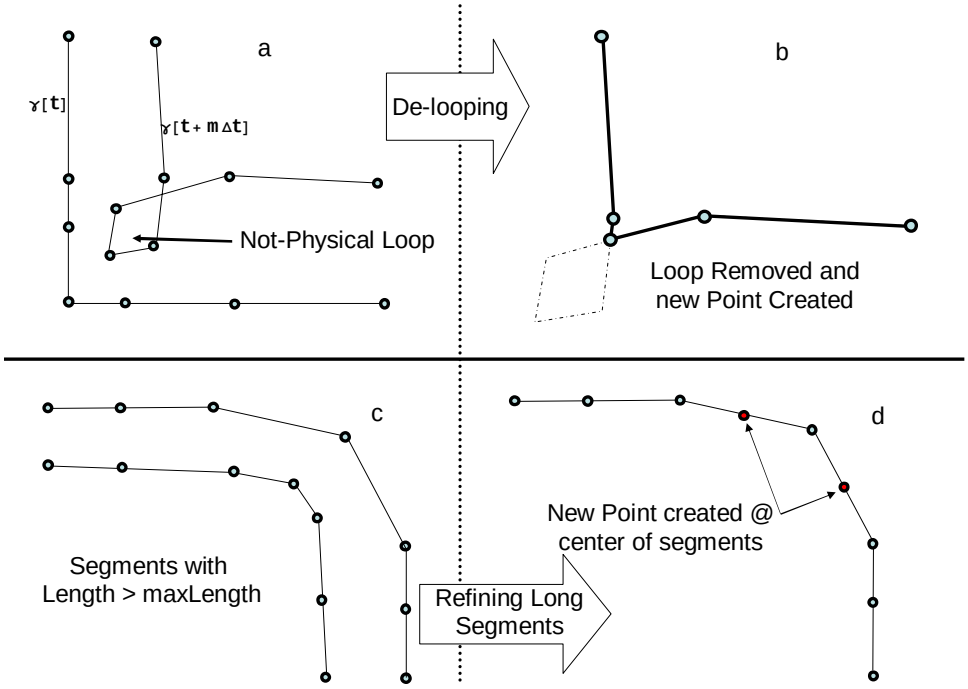

Figure 3: Post-processing after every step of the simple node tracking surface model. 3 a&b illustrate de-looping while c & d illustrate long-segment refinement.

The distortion of the profile due to the movement of the nodes leaves the profile in a state that is sometimes not useable for subsequent deposition rate calculations. The first problem that has to be remedied is the removal of loops that occasionally develop at corners or turns. As can be seen from Figure 3a & 3b, the nodes within the loops have to be removed and a node has to be created at the points of intersection of the segments that create the loop. This de-looping process has to be done after every step and before the profile is used again by the DSMC program to calculate the new flux rate.

Figures 3c and 3d illustrate the other effect that has to be accounted for every step, namely segment stretching at the corners or at areas with gradients in the deposition rate. In our implementation this is accounted for by calculating the lengths of the all segments and splitting in half the ones longer than a pre-specified value *maxLength*. This process ensures that even when a large number of steps are taken, important features like corners and bulges still maintain an acceptable level of detail and model the profile faithfully.

4.2.2 Level Set Method Model

4.2.2.1 Theory

The basic idea behind this method is to regard our boundary as a constant-value (zero) contour of the function ϕ[t,x,y,….] which is defined, in principle, on all points of the computation domain, that is at every point our evolving curve can go. A time-dependent partial differential equation governs ϕ and this determines the movement of the contour boundary. This method was pioneered by Osher and Sethian [9] and has been successfully used in modeling boundaries in a variety of different fields including deposition, image processing, combustion and many others [7][12].

In two dimensions the general equation governing ϕ is:

$$\partial_t \phi[t, x, y] = H[\phi_x[t, x, y], \phi_x[t, x, y]]$$

Here H is the "Hamiltonian" of the problem and depends on the rules that govern the movement of the curve. Furthermore, H can be classified into convex and non-convex depending on the mathematical properties of the function. In the case where the curve moves in a direction normal to its self it can easily be shown that [7] [3]:

$$\partial_t \phi[t, x, y] + F[x, y] \, | \nabla \phi[t, x, y] | = 0 \qquad \textbf{(1)}$$

where F[x,y] a function that determines the normal velocity of the curve and will be discussed in detail in the next section. ϕ is initialized as the signed distance function from the initial boundary. The signed distance function at a point is the distance to the closest point on the curve with a positive or negative sign depending on whether the point is inside or outside the curve.

The LS model is linked to our DSMC code by the using the following steps:

1. Initialize ϕ[t,x,y] as the signed distance function from the initial curve $\gamma^{t=0}$ & set t=0.
2. Run the DSMC code using $\gamma^{t=0}$ and record the flux rate at each segment.
3. Use the flux rate data to build F[x,y] (see § 4.2.2.3).
4. Solve for $\phi[t + \Delta t_{step}, x, y]$ using the numerical scheme outlined in next section (Δt_{step} is the time between calls to DSMC).
5. Use a contour extracting program to get $\gamma^{t+\Delta t_{step}}$ from $\phi[t + \Delta t_{step}, x, y]$.
6. Increment t by Δt_{step}, and repeat steps 2-6 until $t=t_{final}$.

A very important point to keep in mind here is that although we extract the zeroth level contour every time we need to calculate the deposition rate, we never use this contour to re-initialize the values of $\phi[t,x,y]$ at any time. This is done to minimize errors introduced due to finding the contour and then re-initializing $\phi[t,x,y]$ (see section 11.6 of [7] for a more detailed discussion).

We will end this discussion of LS theory by highlighting a special case of Equation (1). When the speed function is always either positive or negative, equation (1) can be re-written in the form (see Chapter 1 of [7] and [2]):

$$|\nabla T[x, y]| F = 1$$

With this formulation the curve at time μ which is normally defined by $\phi[\mu,x,y]=0$ is given by the contour defined by T[x,y]=μ. The big advantage in using this formulation is that one has to solve for T[x,y] only once and then the contour for all times is readily available. This is in contrast with the time dependent LS which in principle requires the integration the full domain of $\phi[t,x,y]$ from initial time to the time μ we are interested in. An other notable advantage for this formulation is that it can be solved very quickly using the Fast Marching Method (FMM) that was developed by Sethian [7][2]. Finally, FMM can be used in the fast calculation of speed functions as explained in §4.2.2.3.

4.2.2.2 Details and Implementation

Osher and Sethian developed a number of numerical schemes to solve the LS equations both for convex and non-convex Hamiltonians [9]. In our implementation we used a second-order convex numerical scheme to integrate $\phi[t,x,y]$. This scheme is designed to properly work even when the derivative function is not well defined as in nodes close to corners and cusps. The basic equation of the scheme is:

$$\phi[t + \Delta t_{num.}] = \phi[t] - \Delta t_{num.} (\mathrm{Max}[F[x, y], 0] \nabla^{+}[x, y] + \mathrm{Min}[F[x, y], 0] \nabla^{-}[x, y])$$

where $\Delta t_{num.}$ is the numerical time step used. Also:

$$\nabla^{+}[x, y] = \sqrt{\mathrm{Max}[A[x, y], 0]^2 + \mathrm{Min}[B[x, y], 0]^2 + \mathrm{Max}[C[x, y], 0]^2 + \mathrm{Min}[D[x, y], 0]^2}$$

$$\nabla^{-}[x, y] = \sqrt{\mathrm{Min}[A[x, y], 0]^2 + \mathrm{Max}[B[x, y], 0]^2 + \mathrm{Min}[C[x, y], 0]^2 + \mathrm{Max}[D[x, y], 0]^2}$$

and

$$A[x, y] = D^{-x}[x, y] + \frac{\Delta x}{2}\, m[D^{-x-x}[x, y], D^{+x-x}[x, y]]$$

$$B[x, y] = D^{+x}[x, y] - \frac{\Delta x}{2}\, m[D^{+x+x}[x, y], D^{+x-x}[x, y]]$$

$$C[x, y] = D^{-y}[x, y] + \frac{\Delta y}{2}\, m[D^{-y-y}[x, y], D^{+y-y}[x, y]]$$

$$D[x, y] = D^{+y}[x, y] - \frac{\Delta y}{2}\, m[D^{+y+y}[x, y], D^{+y-y}[x, y]]$$

$$m[i, j] = \begin{cases} i \text{ if } |i| \le |j| \\ j \text{ if } |i| > |j| \\ 0 \text{ otherwise} \end{cases} \text{ and } ij \ge 0$$

Note that $D^{\pm\eta}[x,y]$ is the forward/backwards difference operator in the η direction and $D^{\pm\eta\pm\eta}[x,y]$ is defined similarly as the second order difference operator. Linear extrapolation is used to find the values of $\phi[t, x, y]$ at points that are outside our domain in the x and y direction.

In our implementation we have elected to solve the equations for the full domain of the problem where ϕ is defined. The Narrow Band method [10] is a method to conserve computational effort by updating ϕ only at points close to the zeroth contour. We have elected not to do so because updating the full 2D domain is very feasible on modern hardware and the time savings would not justify the implementation of the somewhat complicated Narrow Band Method. The size of the numeric step ($\Delta t_{num.}$) that results in converged and stable update of ϕ was determined by a CFL condition and in general less than 10 numeric steps were used between successive calls to the DSMC program to find the surface deposition flux.

An other issue that is critical to the success of this method is the fashion by which the zeroth contour is extracted from ϕ. A relatively fine grid is needed in order to accurately resolve details of the front movement. As [5] shows, a grid of the order of a hundred points is needed in two dimensions to accurately resolve fine or sharp features of the profile to an extent comparable to other methods of modeling the CVD profile. On the other hand an excessively fine profile significantly increases the time needed to get accurate results from the DSMC program. To resolve this dilemma we have found that the most successful approach was to start by producing a very fine mesh that has the same characteristic length of a grid cell. To reduce the number of nodes in the profile, a separate step is performed that removes nodes that do not appreciably change the "shape" of the curve. This is done by calculating the length and angles between successive

segments and removing nodes that do not result in excessively long segments (longer than *maxLength*) or removal of sharp corners (angels >*maxAngle*). Figures 4b & 4c are the results of our node removal procedure when applied to the initial curve shown Figure 4a with two different settings of *maxLength* and *maxAngle*.

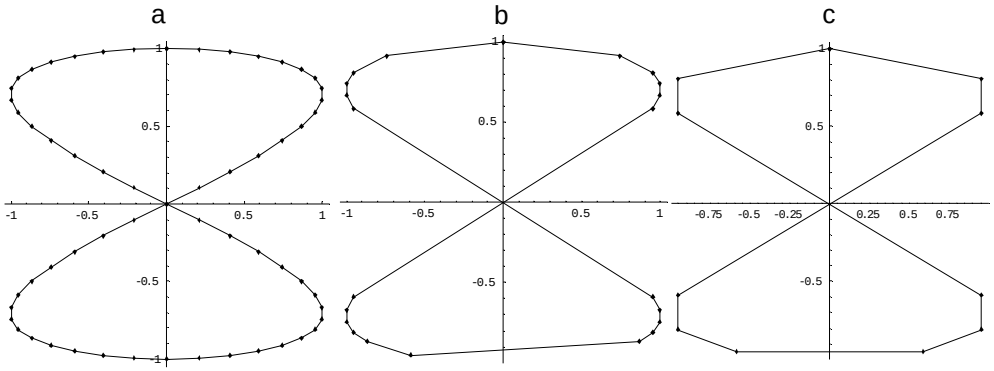

Figure 4: (a) Original detailed curve. (b) Moderate node removal & (c) Aggressive node removal.

In our numerical deposition experiments, successful calculations have resulted from making the maximum allowable segment length 2-4 grid unit lengths. Divergence or convergence to incorrect results was sometimes faced when attempting to allow segment lengths that are significantly higher than this [5].

4.2.2.3 Calculation of Extension Velocities

The deposition rate that we obtain from our DSMC calculation is naturally only meaningful at points along the line segment used in the calculation. A problem that arises from using the LS method is that the speed function F[x,y] in Equation 1 is defined over the *entire domain of* ϕ and not only the deposition curve points. The problem of finding an appropriate F[x,y] given F[γ] (where F[γ] is the flux at point γ on the curve) is complicated and very important to the accuracy of the results and is called the *Extension Problem*. A number of different methods can be used to solve the Extension Problem depending on the details of the front model and are discussed elsewhere ([7] and [5] for example). The method we opted to use is explained in detail in [7] & [6] and uses the FMM to produce an F[x,y] such that $\nabla F[x, y] . \nabla \phi^{temp}[x, y] = 0$ where $\phi^{temp}[x, y]$ is the signed distance function from the deposition curve. This method is essentially equivalent

to assigning each point on the domain the speed function of the closest point on the curve. Points that are equally close to different segments are assigned the average value of the rates of those segments while points on the segments are given velocities that are linearly interpolated from the edges.

4.3 Verification & Examples

In this section we will describe the details of a number of example cases to show that LS can be successfully combined with DSMC to make accurate predictions about deposition profiles. We will start with two simple calculations to verify that our implementation of the LS method does indeed produce accurate results for simple cases. The second set of examples will show how we can reproduce independently verified deposition profiles that have been produced using a very different method.

4.3.1 Simple Examples

The goal of describing the next two examples is to show that our implementation of the LS method can accurately reproduce simple analytical results. The first example is of a circle with an initial diameter of 50 grid points embedded in an array of 200x200 grid points with unit side lengths. The trajectory of the curve is followed by using the second order convex time-integrating scheme introduced in the last section. The integration is done using a constant speed function F[**x,y**] =1 and is plotted in Figure 5a along with the original curve. The color of the final curve represents the distance between the exact solution and the LS solution with lighter colors indicating larger deviations. The maximum deviation is less than 0.384 units which is about 0.8% of the total distance traveled by the curve.

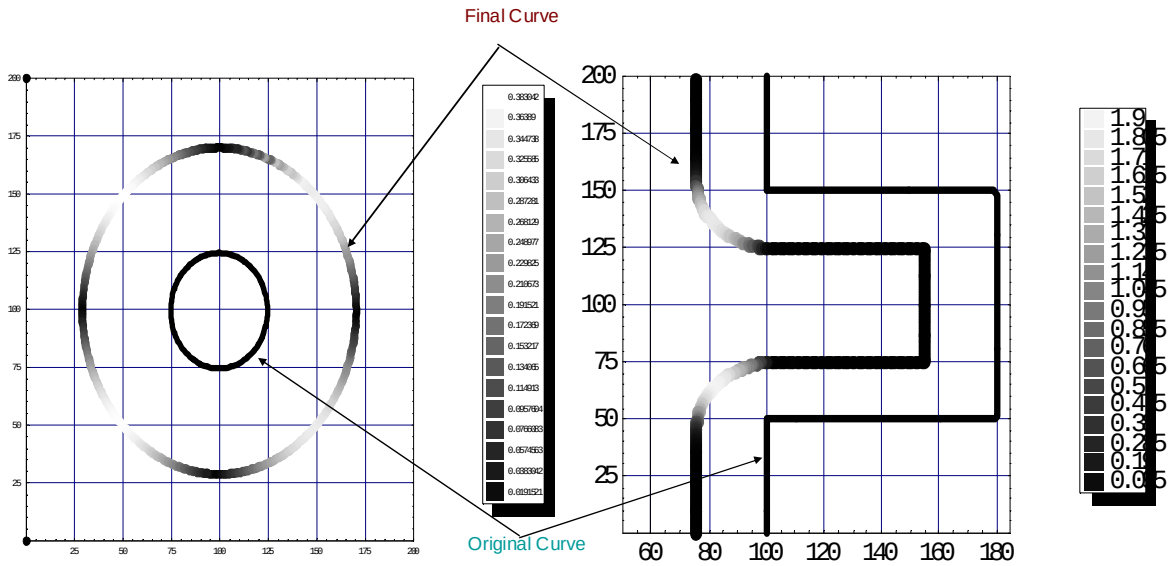

Figure 5: Plot of original profile, final profile and error from exact solution. (a) is a plot of the uniform growth of a simple circle. (b) Plot of uniform growth of more complex curve.

The second example shown in Figure 5b and is identical to the first except for the shape of the initial curve. The initial curve is a series of straight segments and is plotted along with the final curve in a way similar to the last example. The maximum distance between the exact curve and the LS solution is 1.9 units which is about 7% of the distance traveled. The deviation from the exact solution is almost exclusively in the curved area generated from the sharp corner and might be related to the representation of a sharp corner with no rounding.

4.3.2 Verification Examples

The goal of the examples presented in this section is to show that we can successfully combine the LS method with our DSMC program to perform physically accurate CVD simulations. We simulate an infinite trench of width 1 μm and an aspect ratio of 1. The gas pressure is such that we are at the radiation limit (Kn=∞) and we select a sticking coefficient of 0.5. The deposition profile is tracked until the thickness at the surface reaches 0.8 μm. Cale and co-workers show a solution of this specific problem using EVOLVE in [5]. In our work we were able to use both the LS method and our simple node tracking method to accurately track the deposition and reproduce the results of EVOLVE. This confirms that that our DSMC program along with either surface model can produce accurate results as long as the correct parameters are used in the surface model.

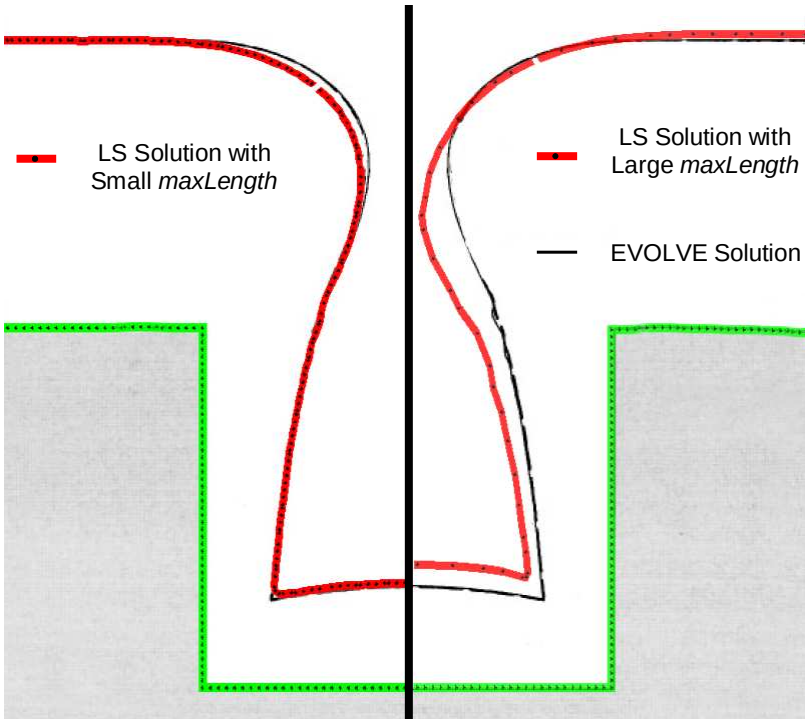

Figure 6: Comparison between converged EVOLVE result with two different CVD solutions using the LS surface model. Left side of figure is for a small maxLength parameter while plot on right is for large maxLength parameter (AR=1, Sc=0.5, Kn→∞, in call cases).

The simplified node tracking model was first used to track the evolution of the deposition front and reproduce the EVOLVE results. The agreement between our calculation and EVOLVE was reasonably good when using 20 separate DSMC deposition rate calculations and a maximum segment length parameter of 3.33units (for a feature width of 100 units). Due to the way the method tracks the nodes the sharpness at the bottom corner is faithfully reproduced which gives a slightly better estimate of the corner step coverage.

The red lines in Figure 6 are the LS results for the same deposition configuration. The red curve on the left results from using the algorithm described in the last section with 40 calls to the DSMC program and using the smoothing algorithm with a *maxLength* of 3 and *maxAngle* of 11.25°. The result is almost identical to the simplified node tracking method and again is in very good agreement with published EVOLVE results.

The results we have gotten from comparing the results of the node tracking method and the LS method is that the latter sometimes needs a significantly larger number of flux evaluations to get converged results. For the LS model any significant reduction of the number of calls to the DSMC program results in significantly inaccurate profiles even with fine *maxLength* and *maxAngle* settings. Efforts to keep the same number of DSMC program calls but with a profile representation that allows larger segment (to reduce the calculation time of DSMC) also results in profiles that have significant inaccuracies in them as can be seen on the right red curve in Figure 6. The use of a different method of calculating the extension velocities (as in [5] and [4]) seems to be the only way of significantly reducing the number of DSMC evolutions needed to get accurate results.

4.4 Optimized Particle Advection Scheme

As pointed out in Chapter 2 there exists a simple method to improve the speed of the particle advection which is effective at lower Knudsen numbers using a simple LS concept. The method relies on having a simple criterion (which does not scale with the number of segments) to judge if a particle will not hit any of the wall segments in the current time step. When this is the case the computational cost of moving a particle goes from O(# of segments) to O(1) which is a substantial saving when the number of segments is large.

The basic idea behind this optimization is to assign to each DSMC cell at the start of the run the distance to the closest point of the closest segment (d_{min}). These values can be found either by a direct minimum distance calculation to all segments or by using the FMM if more speed is required. At the start of the particle movement subroutine the distance to the cell containing the particle is compared to the distance traveled by the particle in the current step. In other words,

$$\Delta t_{DSMC\,Step}\sqrt{v_x^2 + v_y^2} \stackrel{?}{\square} d_{minCell}$$

where $\Delta t_{DSMC\ Step}$ is the time step in the advection part of DSMC.

The only time the particle movement is checked for crossing all the segments is when it travels a distance grater than d_{min} of the cell it started the movement in.

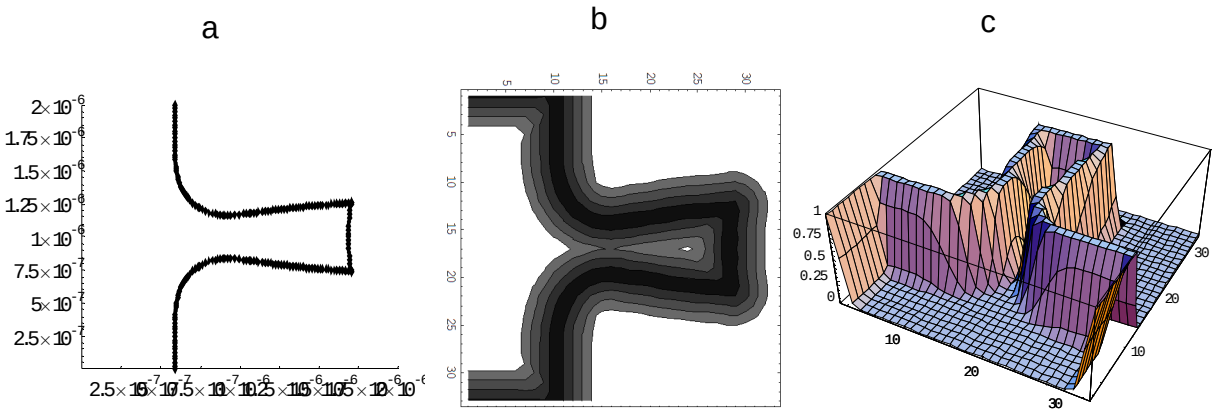

Figure 7: (a) Complex deposition profile with many segments. (b) Plot of isocontours of the distance functions at $\pm\{\tau C, 2\tau C, 3\tau C\}$ (where τ is the mean time between collisions). (c) Fraction of particles at position that have speed grater than d_{min} assuming an equilibrium velocity distribution.

We will try to quantify the savings in time when using the above procedure for the specific case when the Kn=0.05. Figure 7a&b show plots of a deposition profile and the isocontours of the distance function associated with it. Integrating over the Z-Axis component, the equilibrium velocity distribution in the x,y plane is:

$$f[C_x, C_y] = \left(\frac{m}{2\pi kT}\right) e^{\frac{-m(C_x^2+C_y^2)}{2kT}} \quad \Longrightarrow \quad f[r] = \left(\frac{m}{2\pi kT}\right) 2\pi r\, e^{-\frac{mr^2}{2kT}}$$

where $r^2 = C_x^2 + C_y^2$

and hence the fraction of particles with speed C_{min} or higher is

$$S[C_{min}] = \int_{Cmin}^{\infty} f[r]\, dr$$

Hence the fraction of particles in a cell that will travel a distance $d_{min}[x,y]$ or grater in $\Delta t_{DSMC\ Step}$ is $S(d_{min}[x,y]/\ \Delta t_{DSMC\ Step})$ which is plotted in Figure 7c for all cells in the

domain. Furthermore, we can estimate the total fraction of particles that will need to be moved using O(# of segments) steps:

$$\frac{\int\int_{\text{Area of Domain}} S\left[\frac{d_{min}[x,y]}{\Delta t}\right] dx\,dy}{\int\int_{\text{Area of Domain}} 1\,dx\,dy}$$

If we perform the integration for the profile in Figure 7a we find the ratio to be 5%! Table 1 shows a comparison between the simple way of particle advection and the improved way explained above for a simple AR=1 trench. Clearly the improved method is substantially faster and should always be used.

	Kn~0.05	Kn~1	Kn~10
Original Movement Method (s)	148.10	120.06	310.7
Optimized Method(s)	16.18	100.96	319.81
% of time	10.93	84.1	102.9

Table1: Execution time spent in the particle advection subroutine using original algorithm that was explained in Chapter 2 along with improved method presented in this section. The improvement in speed is greatest at lower Kn values. These particular timing results were for 100,000 particles and a profile with 250 segments.

References:

1. Sethian, J and Adalsteinsson, D; *A Fast Level Set Method for Propagating Interfaces.* Journal of Computational physics V. 118 No. 2 269-277 1995.
2. Baerentzen, J A; *On the Implementation of Fast Marching Methods.* IMM Technical Report IMM-REP-2001-13 Technical University of Denmark 2001**.**
3. Hamaguchi, S; *Mathematical Methods for Thin Film Deposition Simulations*. Thin Films V. 22 81 1996.
4. Cale, T, Mahadev, V, Tang, Z, Rajagoplan, G, and Borucki, L; *Topography Evolution During Semiconductor Processing.* Plasma Processing of Semiconductors 109-124 (Williams, PF Ed.) 1997.
5. Richards, D, Broomfield, M, Sen, S and Cale, T ;*Extension Velocities for Level Set Based Surface Profile Evolution.* j. Vac. Sci. Technol. A V. 19 No. 4 Jul/Aug 2001.
6. Adalsteinsson, D and Sethian, J; *The Fast Construction of Extension Velocities in Level Set Methods.* Journal of Computational Physics V. 148 2-22 1999.
7. Sethian, J; *Level Set Methods and Fast Marching Methods: Evolving Interfaces in Computational Geometry, Fluid Mechanics Computer Vision and Materials Science*. Cambridge University Press. 1999.
8. *An Overview of Level Set Methods for Etching Deposition and Lithography Development.* Sethian, J and Adalsteinsson, D, IEEE Transactions on Semiconductor Devices V.10 No.1 167-184 1997.
9. Osher, S and Sethian, J; *Fronts Propagating with Curvature-Dependent Speed: Algorithms Based on Hamilton-Jacobi Formulations.* J. Comp. Phys. V. 79 12-49 1988.
10. Adalsteinsson, D; *Etching, Deposition and Lithography using Level set Techniques,* PhD Thesis University of California at Berkeley 1995.
11. Kim, S; *An O(N) Level Set Method for Eikonal Equations.* SIAM J. Sci. Comput. V. 22 No. 6 2178-2193 2000.
12. Osher,S , Fedkiw, R; *Level Set Methods and Dynamic Implicit Surfaces.* Springer Verlag Publishing 2002.

This Page is Intentionally Left Blank.

CHAPTER 5: CONCLUSION

5.1 Summary

The work presented in this thesis has resulted in an integrated method to capture profile evolution of micro-trenches for a finite time. Our approach is able to obtain results in all Knudsen regimes by incorporating a DSMC method for simulating the gas transport in the feature. Furthermore, we presented a method to account for complex surface chemistry that results in surface sticking coefficients that vary in both space and time. In addition, this work is novel in that it integrates the Level Set surface tracking method with DSMC transport to generate results that have been verified at both the continuum limit and radiation limit. We also used simple concepts from LS theory to significantly improve the performance of the DSMC method at lower Knudsen numbers.

In Chapter 1 we defined chemical vapor deposition for micro-scale trenches, reviewed the special challenges associated with this problem along with some of the previous attempts at solving it for different special cases. We proceeded in Chapter 2 to explain the basic concepts of our methodology and how they are integrated. In addition, Chapter 2 includes a detailed discussion of the unique aspects of our DSMC transport model as well as a discussion of the addition of a non-linear surface chemistry model in our work.

In chapter 3 we present a large number of verification problems. Our results for low pressure deposition were verified by comparing them to analytical formulas as well as published radiation limit solutions. In contrast, we verified problems in the high pressure regime by comparing the deposition profiles to FEA solutions of the continuum diffusion equation. Overall, the agreement between our methodology and other results was satisfactory and indicates the reliability of our approach in modeling CVD. Chapter 3 also presented a number of general trends that show how deposition varies with various transport and deposition parameters. Of particular interest is the conclusion that step coverage worsens as the Knudsen number is reduced.

Chapter 4 discussed two models for trench surface evolution, namely, the Simple Node Tracking model along with the more sophisticated Level Set model. The pitfalls and advantages of each surface model were discussed along with examples which show how they both can produce accurate results when sufficient refinement is used. We concluded chapter 4 with an explanation of a fairly simple method to dramatically improve the performance of the particle advection part of the DSMC when dealing with complex walls using level set concepts.

5.2 Possible Extensions of This Work

The first and most obvious area where this work can be extended is to use our methodology to deal with 3D trenches and structures. Conceptually this is straightforward because both the DSMC transport model and the Level Set surface model can extended easily to the 3rd dimension. A number of modern DSMC codes with complex geometries have been developed and used extensively in aerospace engineering[1] and other fields [3][2]. The extension of the level set surface model is trivial and has already been applied successfully to a number of ballistic transport flows [4][5][8]. Reference [8] shows an example where the solution of the 3D deposition problem enables the prediction of complex surface phenomena that may not be evident from solutions of 2D problems.

One limitation with the current implementation of the DSMC transport model is that it requires a very long time to give meaningful deposition results in cases where the reactive species has a low concentration. This is due to the statistical nature of the DSMC method which requires many particle collisions with a surface in order to have a good estimate of the deposition rate on that surface. The use of different weighting factors for each species to improve the results for the low concentration species is a possible method for dealing with the problem. Weighting factors are discussed in [9] and more recently in [6] and in fact, have been incorporated in our DSMC transport model but have neither been verified to give accurate results nor used in the examples presented.

There are a number of other interesting questions with relation to how the Level Set surface model is integrated with the transport model and methods of sharing information between them in more natural ways. A simple example might be the use of the DSMC cell molecular flux instead of the current velocity extension routine to improve the speed of the calculation by requiring fewer transport model calls. Another (more ambitious) prospect in integrating the two methods would be to attempt to directly use the level set information in the DSMC model without explicitly finding the segments that represent that boundary.

It would also be interesting to investigate if the performance of the particle advection

subroutine can be significantly improved any further by using LS information. One possibility is to maintain a sorted list of distances between DMSC cells and segments of the boundary. Only segments that have a distances smaller than the distance traveled by the particle in the current time step are considered for collisions and then in the order of their distance. An alternative wall collision detection approach could be to use visibility ideas discussed by Sethian on visibility calculations using the distance function that does not scale with the number of segments that represent the trench boundary [7].

References:

1. LeBeau, GL; *A Parallel Implementation of the Direct Simulation Monte Carlo Method.* Computer Methods in applied Mechanical Engineering V. 174 319-337 1999.
2. Bird, GA; *Molecular Gas Dynamics and the Direct Simulation of Gas Flows.* Oxford University Press 1998.
3. Coronell, DG; *Simulation and Analysis of Rarefied Gas Flows in Chemical Vapor Deposition Processes.* PhD Dissertation MIT 1993.
4. Adalsteinsson, D and Sethian, J; *A Level Set Approach to a Unified Model for Etching, Deposition, and Lithography II: Three-Dimensional Simulation*. V. 122 No. 2, 348-366 1995.
5. Cale, T, Mahadev, V, Tang, Z, Rajagoplan, G, and Borucki, L; *Topography Evolution During Semiconductor Processing.* Plasma Processing of Semiconductors 109-124 (Williams, PF Ed.) 1997.
6. Boyd,I D ;*Conservative Species Weighting Scheme for the Direct Simulation Monte Carlo Method.* Journal of Thermophysics and Heat Transfer, V. 10 No. 4 October-December 1996.
7. Sethian, J; *Level Set Methods and Fast Marching Methods: Evolving Interfaces in Computational Geometry, Fluid Mechanics Computer Vision and Materials Science*. Cambridge University Press. 1999.
8. Adalsteinsson, D and Sethian, J; *A Level Set Approach to a Unified Model for Etching Deposition and Lithography III: Re-deposition, Re-emission Surface Diffusion and Complex Simulations.* j. comp. phys. V. 138 No. 1 193-223, 1997.
9. Bird, G; *Molecular Gas Dynamics,* Clarendon Press, Oxford 1976.